

POLITECNICO DI TORINO

Collegio di Ingegneria Energetica e Nucleare

Corso di Laurea Magistrale in Ingegneria Energetica e Nucleare

Tesi di Laurea Magistrale

**A TECHNO-ECONOMIC FEASIBILITY STUDY OF A HYBRID
RENEWABLE PLANT FOR HYDROGEN PRODUCTION AND
TRANSPORTATION IN THE EXISTING GAS PIPELINES:
A CASE STUDY IN ALGERIA**



Relatore

Prof. Pierluigi Leone

Co-relatore

Enrico Vaccariello

Candidata

Giulia Carrara

Ottobre 2019

ABSTRACT

Hydrogen is considered one of the most interesting energy carriers of the future: its clean production from Renewable Energy Sources (RES hydrogen) and its transportation options are two of the main topics of the “Hydrogen Economy”. The electrical energy provided from renewable sources can be transported either as electricity or can be transformed into a secondary energy carrier, as the hydrogen: in both cases, it is required a specific infrastructure in order to transfer the “energy product” from the generation site to the demand site. As the energy demand of the Central Europe is high, but its renewable energy potential is moderate if compared to other regions such as North Africa, an interesting compromise to analyse is generating energy in these regions with a higher renewable potential and importing it to areas with a higher energy demand.

In this thesis work, a techno-economic feasibility study of a hybrid renewable plant, located in Hassi R'Mel (Algeria), is performed. The analysed hybrid plant is composed by a large-scale PV-WIND-STORAGE system: the energy generated from the plant is used to work an electrolysers-system for producing renewable hydrogen. The produced hydrogen (H_2) is sent as a blend, in a specific percentage, with the natural gas (NG) through the existing pipelines towards Southern Europe. This work mainly consists of the following parts: the design of each sub-system forming the hybrid plant, an optimization analysis with *MATLAB Software* in order to find the best configuration, in terms of LCOE, of the hybrid plant and the estimation of the unit cost of the produced hydrogen with the proposed hybrid system.

Index

| | |
|--|-----------|
| 1. Introduction | 8 |
| 2. The Algerian energetic context | 9 |
| 2.1 Algeria as producer and exporter of conventional hydrocarbons..... | 9 |
| 2.1.1 Natural gas demand and supply in Italy | 11 |
| 2.1.2 The Transmed Pipeline: characteristics and transport capacity | 14 |
| 2.1.3 Hydrogen transport through pipelines | 16 |
| 2.2 The Renewable potential of Algeria..... | 18 |
| 2.3 Algerian hydrogen potential from renewable energy | 22 |
| 2.4 Hassi R'Mel: Integrated Solar Combined Cycle (ISCC) power plant..... | 24 |
| 3. Technical feasibility of a hybrid system for the hydrogen production: Case study | 25 |
| 3.1 Geographical and Meteorological Characteristics of the site | 25 |
| 3.2 Design of the hybrid plant's sub-systems: Mathematical Models | 28 |
| 3.2.1. Wind System..... | 29 |
| 3.2.1.1 Wind distribution from measured data | 33 |
| 3.2.1.2 Weibull Probability density function..... | 35 |
| 3.2.1.3 Comparison between the two approaches | 40 |
| 3.2.2 PV System | 41 |
| 3.2.3 Storage System..... | 45 |
| 3.2.4 Electrolysers' System..... | 48 |
| 4. Optimization analysis of the hybrid system | 51 |
| 4.1 Calculation method for the Storage system's nominal capacity | 53 |
| 4.2 "Levelized Cost of Electricity" (LCOE) of the different configurations..... | 58 |
| 4.3 "Levelized Cost of Hydrogen" (LCOH ₂) | 65 |
| 5. Conclusions | 70 |
| 6. References | 71 |
| APPENDIX A: Matlab code | 74 |

List of Figures

- Figure 1: Total Primary Energy Supply (TPES) by source, Algeria (1990-2016) [1]9
- Figure 2: a) Natural gas final consumption b) Oil products final consumption, Algeria (2016) [1]10
- Figure 3: Share of Algerian electricity generation by fuel, 2016 [1]10
- Figure 4: Share of Italian electricity generation by fuel, 2016 [1]12
- Figure 5: Italian natural gas imports (2017) [4]13
- Figure 6: Monthly distribution of natural gas imports (2017), "Own elaboration from [4]" ...13
- Figure 7: Gas Pipelines Network from North Africa to Central Europe [7]15
- Figure 8: "Activity" of the Transmed Pipeline, "Own elaboration from [4]"15
- Figure 9: Wobbe-index behavior with different H₂-NG mixtures [39]17
- Figure 10: Algeria.....18
- Figure 11: Electricity generation from renewable sources, Algeria (1990-2016) [1].....19
- Figure 12: Objectives of renewable energy production program in Algeria by 2030 [12]20
- Figure 13: Overall daily average exposure received in Algeria [8].....21
- Figure 14: Wind chart of Algeria [8]21
- Figure 15: Comparison of solar and wind hydrogen production in Algeria [12]23
- Figure 16: ISCC power plant of Hassi R'Mel.....24
- Figure 17: Hassi R'Mel (33.0120N/2.9878E) from Meteonorm 7.3 Software25
- Figure 18: Monthly Solar Irradiation of the Site26
- Figure 19: Monthly Wind Speed at height of 10 m27
- Figure 20: Wind Frequency Distribution at 10 m27
- Figure 21: Scheme of the Hybrid System.....28
- Figure 22: Cp vs. TSR of WTs [18]29
- Figure 23: Manufacturer characteristic (Power) Curve of the selected WT [17]29
- Figure 24: Monthly Wind Speed at hub height (105 m) vs. Monthly Wind Speed at reference height (10 m).....32
- Figure 25: Hourly Energy produced by the WT in a year.....34
- Figure 26: Monthly Energy production of WT34
- Figure 27: Weibull probability density function in terms of hours per year38
- Figure 28: Weibull probability function and WT's Power curve38
- Figure 29: View of the PV-GIS Software operational window41
- Figure 30: Hourly Energy Production of the PV panel.....44
- Figure 31: Monthly Energy Production of the PV panel.....44
- Figure 32: Flow Chart of the Storage system's model.....47
- Figure 33: Flow Chart of the generated computer code with Matlab Software56
- Figure 34: Global LCOE of utility-scale renewable power generation technologies, 2010-2018 [35].....59
- Figure 35: Global weighted average total installed costs and project percentile ranges for same renewable technologies [35]60
- Figure 36: Battery price by type for utility-scale applications [36].....61
- Figure 37: Percentage of the Total Costs of the Optimal PV-WIND-STORAGE SYSTEM configuration.....63

Figure 38: Monthly energy production of the optimal hybrid system.....63
Figure 39: Evolution of the State of Charge (SOC) of the Optimal Configuration64
Figure 40: The LCOE for projects and global weighted average value [35].....65
Figure 41: Percentage of the Total Costs of the whole hybrid plant66
Figure 42: Influence of STORAGE costs on LCOH267
Figure 43: Cost of hydrogen as a function of cost of electricity and utilisation rate of PEM electrolyser [37]68
Figure 44: Hybrid solar and wind load factors [38]69

List of Tables

| | |
|---|----|
| Table 1: Natural gas and oil demand of Algeria [2]..... | 11 |
| Table 2: Natural gas and crude oil exports of Algeria [2] | 11 |
| Table 3: Natural gas imports of Italy [2] | 12 |
| Table 4: Infrastructure modifications according to the hydrogen injection rate | 18 |
| Table 5: Distribution of installed power per resources [10] | 20 |
| Table 6: Technical Data of the selected WT [17] | 30 |
| Table 7: Obtained values because of the wind speed variations with height | 32 |
| Table 8: Annual energy produced by the WT, WT's Capacity factor (C_f) and WT's equivalent hours (h_{eq}) | 35 |
| Table 9: Weibull's annual average parameters | 37 |
| Table 10: Values for the calculation of the WT energy production | 39 |
| Table 11: Annual energy produced by the WT, WT's Capacity factor (C_f) and WT's equivalent hours (h_{eq}) | 39 |
| Table 12: Comparison between the two approaches | 40 |
| Table 13: Results obtained by PV-GIS for 0.3 kW of installed peak PV power | 41 |
| Table 14: Technical Data of the selected PV panel [24] | 43 |
| Table 15: SOC_{max} and SOC_{min} of the considered Storage system | 46 |
| Table 16: Parameters used for the mathematical model..... | 47 |
| Table 17: Datasheet of the selected Li-ion battery [26]..... | 47 |
| Table 18: The required amount of hydrogen for its transportation in pipeline | 49 |
| Table 19: Results obtained for the Load demand | 50 |
| Table 20: Monthly energy production..... | 52 |
| Table 21: Configurations analysed of the hybrid plant | 52 |
| Table 22: Daily mismatch computed for each of the 11 configurations | 54 |
| Table 23: Nominal Capacity of the STORAGE SYSTEM for each configuration..... | 57 |
| Table 24: Considered costs for the calculation of LCOE of the PV-WIND-STORAGE SYSTEM.. | 61 |
| Table 25: LCOE of the 11 analysed configurations of the hybrid plant..... | 62 |
| Table 26: LCOE of the only WT and PV SYSTEM..... | 64 |
| Table 27: Costs of PEM Electrolysers' system [15]..... | 66 |
| Table 28: Levelized Cost of Hydrogen ($LCOH_2$) produced by the proposed hybrid plant | 66 |
| Table 29: Levelized Cost of Hydrogen ($LCOH_2$) per unit of produced kg by the proposed hybrid plant..... | 67 |

1. Introduction

The main feature of Hybrid Renewable Energy Systems (HRES) is to combine two or more renewable power generation so that is possible to address the reliability, efficiency, emissions and economical limitations of a single renewable energy source. In particular, the HRES are popular and frequently used in off-grid applications, for isolated areas.

In this thesis, an off-grid hybrid plant powered by solar and wind resources has been analysed and designed for the generation of a specific amount of hydrogen via electrolysis process. The combination of the solar and wind resources permits to improve the problem related to the intermittent energy production of a singular renewable source. The solar resource, in fact, is more available during summer months and during the winter's sunlit days, while the wind is more available during the winter months and the night. For these reasons, with a hybrid PV-WIND energy system is possible to obtain a more stable energy production during the year than either solar or wind-only systems. Furthermore, the designed hybrid PV-WIND plant considers also a large-scale STORAGE system composed by battery banks in order to supply the energy required by the electrolysers' system (load demand) during the hours in which the energy production of the hybrid renewable system is lower than the load demand.

The designed renewable plant has been located in North Africa (Algeria) due to its high potential in terms of solar and wind resources and also because, at the moment, four pipelines are in operation between North Africa and Southern Europe to deliver natural gas (NG) or, as in this case study, a potential natural gas-hydrogen blend (NG-H₂ blend). The four pipelines are:

- **Magreb Europe Gas (MEG)** connecting Algeria and Spain via Morocco;
- **Medgaz** connecting Algeria and Spain directly;
- **Transmed** connecting Algeria and Italy via Tunisia;
- **Greenstream** connecting Libya and Italy directly.

The first three pipelines exporting natural gas to Europe start in Hassi R'Mel (Algeria) and so, also for economic reasons related to the transport costs of the produced hydrogen, the designed hybrid renewable plant has been placed in that area.

In this case study, the hybrid plant has been sized according to the natural gas transport capacity of the only **Transmed** pipeline and has been chosen a hydrogen percentage (in the NG-H₂ blend) of 2%vol. The reasons behind these choices will be discussed and explained in the following sections of the work.

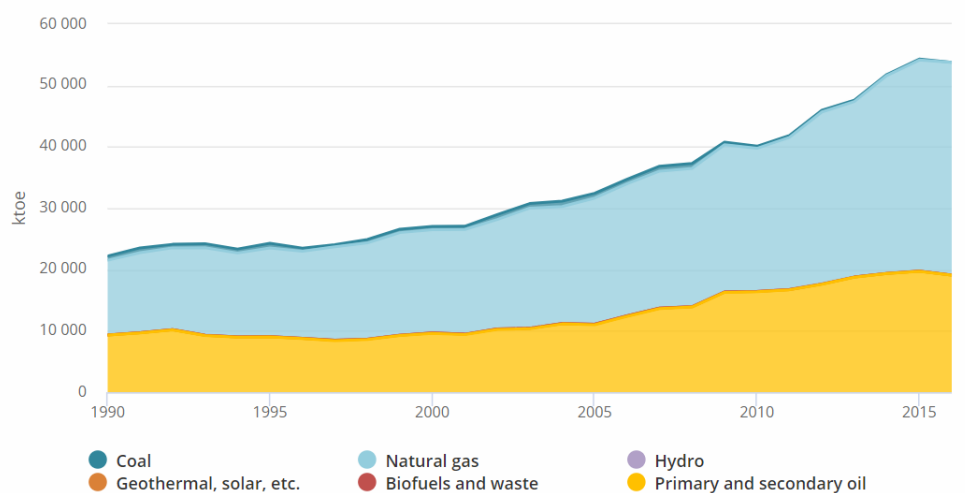
Moreover, in order to obtain a hybrid PV-WIND-STORAGE system able to meet, for each hour of the year, the energy required by the electrolysers' system with the lowest Levelized Cost of Electricity (LCOE), an optimization analysis has also been performed with *MATLAB Software*. Finally, the unit cost of the produced hydrogen with the proposed hybrid system has been estimated.

2. The Algerian energetic context

In this section, a brief overview of the Algerian energetic context is illustrated. In particular, has been analysed the importance of the hydrocarbons in the Algerian energetic mix and their production, consumption and exports especially towards Italy. Furthermore, it has been discussed the possibility of transporting hydrogen through the natural gas pipelines' network, the energy transition of the Country towards a renewable energy production and the Algerian potential for hydrogen generation.

2.1 Algeria as a producer and exporter of conventional hydrocarbons

In the Algerian energetic mix, the hydrocarbons play a crucial role: the Algerian economy is highly dependent on the gas and oil sector due to the presence, in the Country, of large reserves (12.2 billion barrels of oil and 4.5 billion cubic meters [2])¹. According to the statistics of the “International Energy Agency” (IEA), between the 1990-2016, the Total Primary Energy Supply (TPES) of Algeria has increased by more than 150%. New energy needs were mainly met by natural gas, primary and secondary oil, while only a small portion of TPES was provided by coal and renewable sources.



IEA World Energy Balances 2018

* TPES here excludes electricity and heat trade

Figure 1: Total Primary Energy Supply (TPES) by source, Algeria (1990-2016)² [1]

¹ They are the proven hydrocarbons reserves of Algeria, but the potential is probably higher because the Country has not been totally explored.

² Toe (“Tonne of oil equivalent”), is a unit of energy defined as the amount of energy released by burning a tonne of crude oil. The exact value of 1 toe is defined by convention due to the different caloric values of crude oils. The International Energy Agency (IEA) defines 1 toe equals to 11.63 MWh or 41.868 GJ.

Among the Africa’s Countries, Algeria is the largest producer of the natural gas and it is also in the top three oil producers. The gas and oil alone provide more than a third of Gross Domestic Product (GDP)³, 70% of the government revenue and nearly 98% of total exports [2].

The Algerian final consumption of natural gas (**Fig. 2.a**) in 2016, was mainly related to the residential sector, while in the case of oil products (**Fig. 2.b**), the principal interested sector was the transport one.

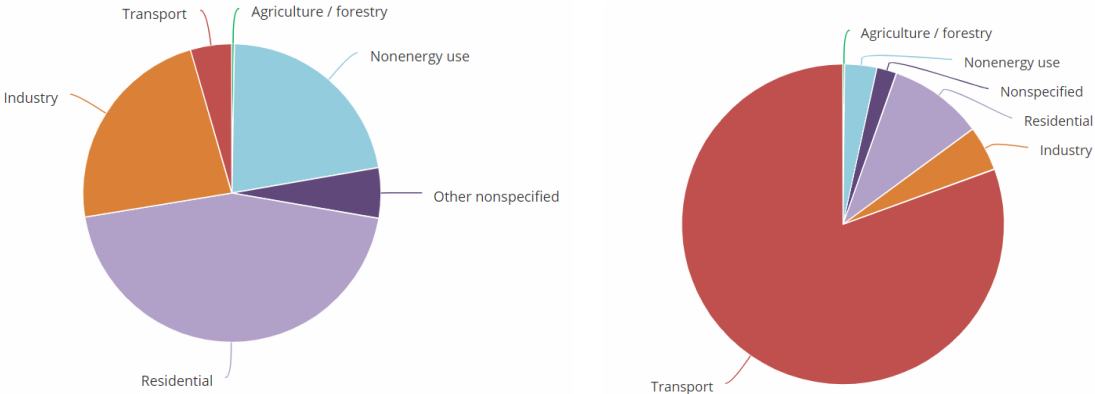


Figure 2: a) Natural gas final consumption b) Oil products final consumption, Algeria (2016) [1]

It is possible to see (**Fig. 3**) how the Algerian electricity generation is totally based on natural gas, 97% of the installed power, while only a small contribution is given by the oil and the renewable sources: hydropower, solar PV and wind.

In Algeria, the totally electricity consumption, from 1990 to 2016, sharply increased from 13.69 TWh (1990) to 60.07 TWh (2016) [1] due to demographic, urban and economic development in constant progression.

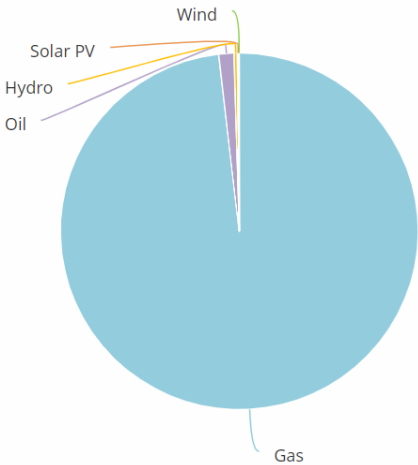


Figure 3: Share of Algerian electricity generation by fuel, 2016 [1]

³ GDP (“Gross Domestic Product”), is a monetary measure of the market value of all the final goods and services produced in a specific time period, often annually. The GDP is the Italian PIL.

Among the African Countries, the Algerian natural gas demand (58.74 bcm in 2017) is the highest after Egypt while, in case of oil, Algerian demand is the third among the African Countries after Egypt and South Africa.

In order to have an idea of the natural gas and oil demand of Algeria, values from 2013 to 2017, have been collected in the following tables.

| NATURAL GAS DEMAND [bcm] | 2013 | 2014 | 2015 | 2016 | 2017 | % CHANGE 17/16 |
|---------------------------------|-------------|-------------|-------------|-------------|-------------|-----------------------|
| Algeria | 36.66 | 37.50 | 39.02 | 39.55 | 40.37 | 2.1 |
| OIL DEMAND [barrels/day] | | | | | | |
| Algeria | 377 000 | 389 000 | 419 000 | 399 000 | 422 000 | 5.6 |

Table 1: Natural gas and oil demand of Algeria [2]

According to the “*Organization of the Petroleum Exporting Countries (OPEC): Annual Statistical Bulletin (2018)*”, the natural gas production of Algeria (in 2017) amounted to 94.78 bcm, while the average daily oil production (in 2017) was 1058700 of barrels. Analysing the values of natural gas and oil demand and production of Algeria, it is clear the high potential of the Country as hydrocarbons exporter. In the following tables, the amount of the Algerian exported natural gas and (crude) oil have been reported.

| NATURAL GAS EXPORTS [bcm] | 2013 | 2014 | 2015 | 2016 | 2017 | % CHANGE 17/16 |
|--|-------------|-------------|-------------|-------------|-------------|-----------------------|
| Algeria | 46.71 | 44.19 | 43.42 | 53.98 | 53.89 | -0.2 |
| CRUDE OIL EXPORTS [barrels/day] | | | | | | |
| Algeria | 744 000 | 622 900 | 642 200 | 668 300 | 632 600 | -5.3 |

Table 2: Natural gas and crude oil exports of Algeria [2]

2.1.1 Natural gas demand and supply in Italy

Italy is characterized by a strong energy dependency on external supply: the 76% of the consumed energy is imported. In the European Union, only other six Countries presents an external energy dependency higher than the Italy: Cyprus (imports the 98% of energy), Malta (imports the 97% of energy), Luxemburg (imports the 96% of energy), Ireland (imports the 89% of energy), Belgium (imports the 84% of energy) and Lithuania (imports the 78% of

energy)⁴ [3]. Some of the main causes related to the Italian energy dependency on external supply are either its poor presence of hydrocarbons deposits in the territory and the absence of nuclear energy. Italy imports the 90% of its natural gas demand for the industry, heating, transport and electrical energy production [4].

The Italian natural gas imports, production and demand, from 2013 to 2017, are showed in the following table.

| NATURAL GAS IMPORTS ⁵ [bcm] | 2013 | 2014 | 2015 | 2016 | 2017 | % CHANGE 17/16 |
|---|-------|-------|-------|-------|-------|-------------------|
| Italy | 61.95 | 55.76 | 61.2 | 65.29 | 69.62 | 6.6 |
| NATURAL GAS PRODUCTION [bcm] | | | | | | |
| Italy | 7.73 | 7.15 | 6.77 | 5.78 | 5.54 | -4.2 |
| NATURAL GAS DEMAND [bcm] | | | | | | |
| Italy | 70.06 | 61.91 | 67.52 | 70.91 | 75.15 | 6.0 |

Table 3: Natural gas imports of Italy [2]

In Italy, in fact, if the contribution of the renewable sources for the electricity generation is relevant, especially if compared to that of Algeria (compare **Fig.3** and **Fig.4**), the situation is different for the industry, heating and transport sector where the natural gas plays an important role: this explains the high Italian natural gas demand and its necessary importation from other Countries.

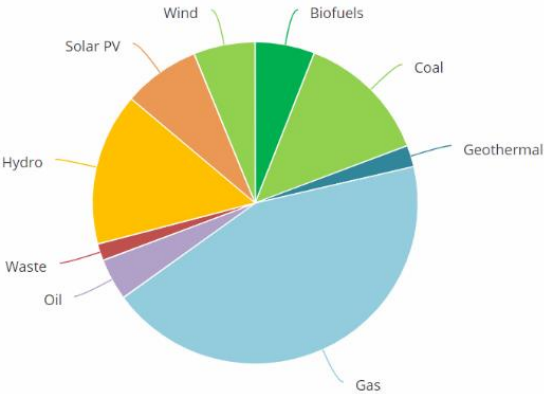


Figure 4: Share of Italian electricity generation by fuel, 2016 [1]

⁴ The energy dependency rates are referred to the year 2015. Among the five Member States consuming the largest amounts of energy, the least dependent on energy imports were the United Kingdom (37.4%) and France (46.0%), in contrast to Germany (61.9%), Spain (73.3%) and Italy (77.1%).

⁵ In 2018, the Italian natural gas import was 67.88 bcm so it decreased respect to the 2017 (-2.6 %). In Italy, the minimum and maximum values of natural gas import were registered in 1975 (8.74 bcm) and 2006 (77.40), respectively [5].

The largest supplier of natural gas to Italy is Russia, the only other partners with a significant share in the Italian natural gas imports are Algeria, Qatar and Libya. The values of natural gas imports of 2017 are showed in **Figure 5**.

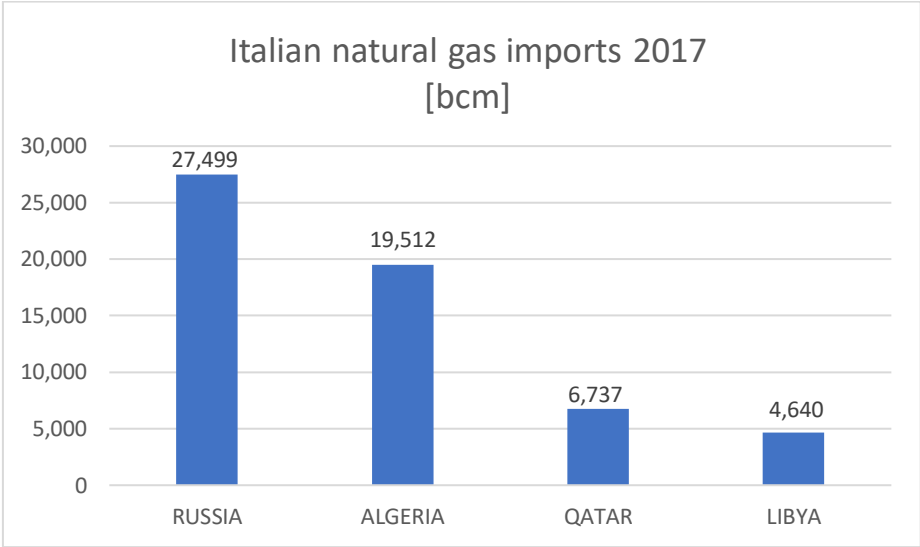


Figure 5: Italian natural gas imports (2017) [4]

According to the “Italian Ministry for Economic Development”, Russia accounted for 39.5% of the Italian natural gas import in 2017, while Algeria accounted for 28% of the Italian gas import (2017).

In **Figure 6** it is possible to see the monthly distribution (in 2017) of natural gas supply by Russia and Algeria: of course, it increases during the winter months due to the higher heating demand [3].

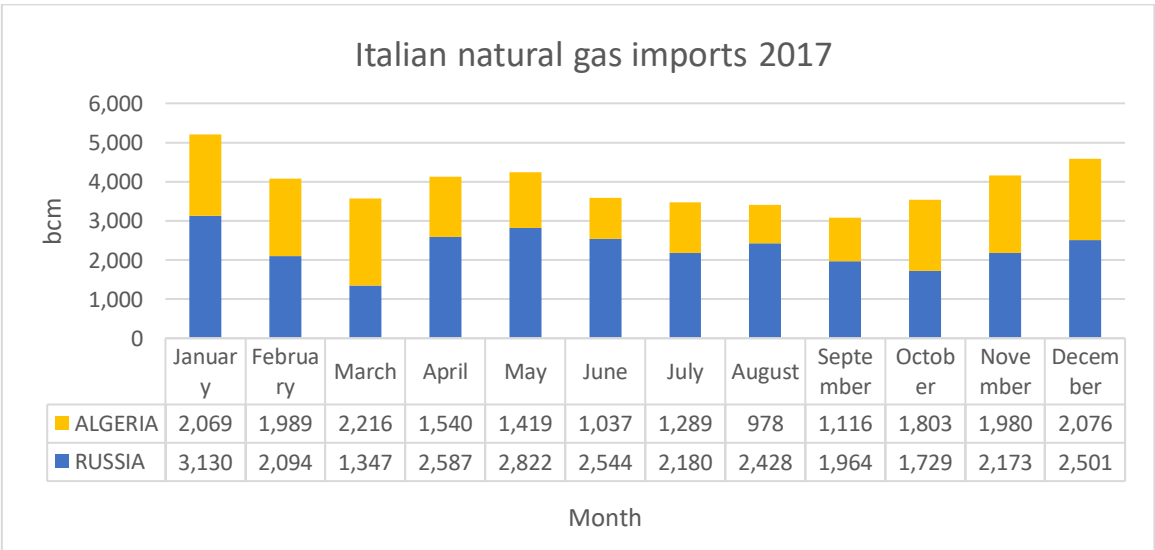


Figure 6: Monthly distribution of natural gas imports (2017), “Own elaboration from [4]”

From these data and statistics, it is evident the importance of Russia and Algeria for the Italian energy economy. In the following discussion, a description and analysis of the **Transmed** pipeline has been developed, since it is of fundamental interest for this techno-economic study.

2.1.2 The Transmed Pipeline: characteristics and transport capacity

The Trans Mediterranean Pipeline (**Transmed**), known also as Enrico Mattei's pipeline, is an important pipeline built in 1983 and connecting Algeria with Italy passing through Tunisia.

The Transmed pipeline is connected to the Hassi R'Mel gas field, the largest onshore gas field in Algeria, producing 2000 bcm/year. The Italian import point is Mazara del Vallo (Sicily).

The total length of the pipeline, from Hassi R'Mel to Minerbio (Bologna), is approximately of 2500 km: 550 km in Algeria, 370 km in Tunisia (TTPC, "Trans Tunisian Pipeline Company"), 160 km in Strait of Sicily and 1420 km on the Italian territory.

The pipeline was realized with a diameter of 48" ⁶, except for the Strait of Sicily and Messina where two lines of 20" were placed and in the last 320 km until to Minerbio where a pipe's diameter of 42" was located.

Along the 2000 km of the pipeline, nine compressor stations have been installed: one in the Algerian section, three in Tunisian section, one in Sicily and four in Italy section [6].

The Transmed is the longest international gas pipeline system: the first pipeline project (1978-1983) included a pipeline with a supply capacity of 12.3 bcm/year, in these years Eni and Sonatrach⁷ firmed the first contract for a gas supply period of 25 years. In 1997, thanks to the construction of a second line, the transport capacity of the pipeline was increased up to 24 bcm/years.

Now, the total transport capacity of the Transmed reaches 33 bcm/year.

⁶ 1 inch is equal to 2.54 cm.

⁷ Sonatrach is the Algerian State Authority operates the Algerian section of the gas pipeline, while the Tunisian section is owned and controlled by Sotugat and Sergaz respectively. The channel of Sicily is controlled by Trans-Mediterranean Pipeline Company (TMPC), a joint venture of Eni and Sonatrach. Snam Rete Gas, a subsidiary of Eni, operates the Italian section.

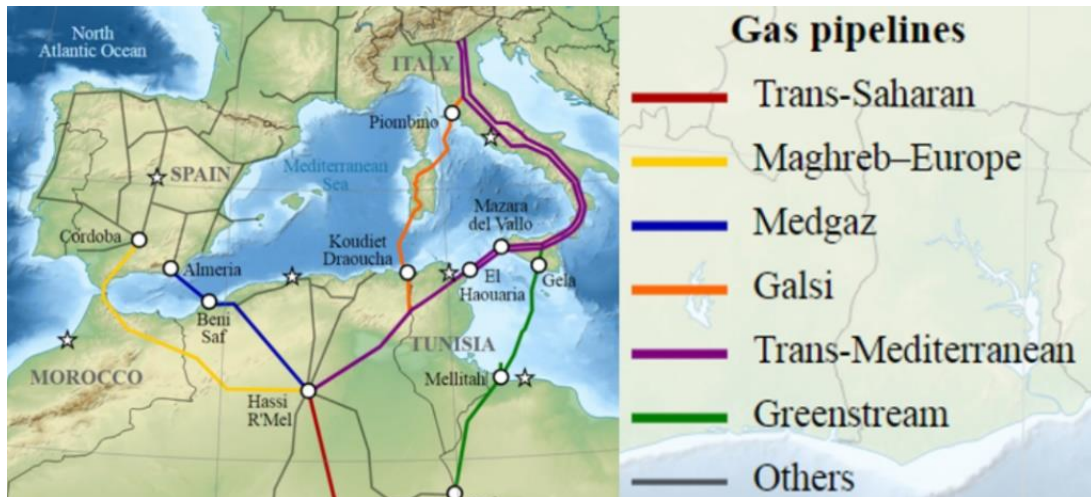


Figure 7: Gas Pipelines Network from North Africa to Central Europe [7]⁸

In order to evaluate the “activity” of the Transmed pipeline, during the years (2010-2017), which means the amount of natural gas transported from Algeria (Hassi R’Mel gas field) to Italy, a histogram has been reported as a result of the analysis of data and statistics of “Italian Ministry for Economic Development”.

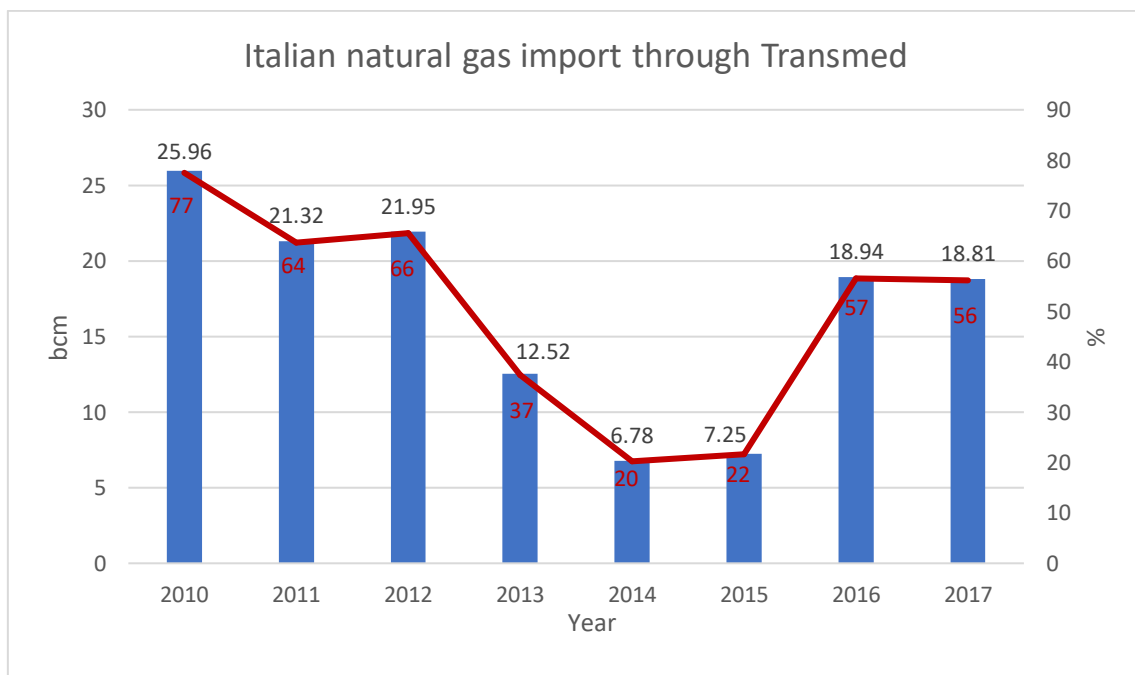


Figure 8: “Activity” of the Transmed Pipeline, “Own elaboration from [4]”

During the analysed period, 2010 represents the year with the highest gas import through the Transmed pipeline (equals to 77% of the total transport capacity of the pipeline), while the

⁸ At the moment, the Galsi pipeline is not in operation.

years with the lower values are the 2014 and 2015: in 2014, only the 20% of the total transport capacity has been exploited.

In the analysis, a general decrement in the natural gas import (through the Transmed pipeline) can be noticed.

The “activity” analysis of the Transmed pipeline is important, for this work, because some of the main assumptions made for the techno-economic feasibility study of the hybrid plant, object of the work, are based on these statistics. In particular, the hybrid plant has been sized considering that only the 70% of the total transport capacity of the Transmed pipeline is exploited (during the years, it has never been exploited at full transport capacity).

2.1.3 Hydrogen transport through pipelines

The existing NG transport network mainly consists of:

- Pipelines;
- Compression stations;
- Pressure-reduction stations.

This network serves to transport a sufficient amount of energy towards any end-user, but it is also used to store NG whenever the gas supply exceeds the demand. This (short-term) storage of NG in pipelines is called “linepack”, which allows an almost continuous supply of NG into the network, despite a strongly fluctuating demand pattern.

Among the different options for the hydrogen transport, the utilization of the existing natural gas network appears the most economically viable. In general, based on research to date, only minor issues arise with blends of less than 5%–15% hydrogen (by volume), depending on site-specific conditions and particular natural gas compositions. More significant issues must be addressed for higher blends in the range of 15%–50%, such as conversion of household appliances or an increase in compression capacity along distribution mains serving industrial users. Blends above 50% face more issues across multiple areas, including pipeline materials, safety, and modifications required for end-use appliances or other uses. In particular, mixing of higher percentages of hydrogen into the natural gas produces effects on the:

- “Linepack”;
- Pressure drop;
- Wobbe-index.

The Wobbe-index is a measure for exchangeability of gases in gas burners, and consequently determines whether they can be used in domestic applications. It is calculated as follows [40]:

$$W_s = \frac{HHV}{\sqrt{d}}$$

Where

W_s : is the Wobbe-index;

HHV : is the Higher Heating Value, [MJ/Nm³];

d : is the relative density compared to air, [-].

The boundaries within which the Wobbe number must lie for common rich NG burners are 48 and 58MJ/Nm³. When lean NG is used in standard burners, the Wobbe number has to lie between 41 and 47MJ/Nm³. From the following figure, it can be seen that for lean NG burners, up to 98 vol% of hydrogen can be added, while for rich NG, up to 45vol% of hydrogen can be injected.

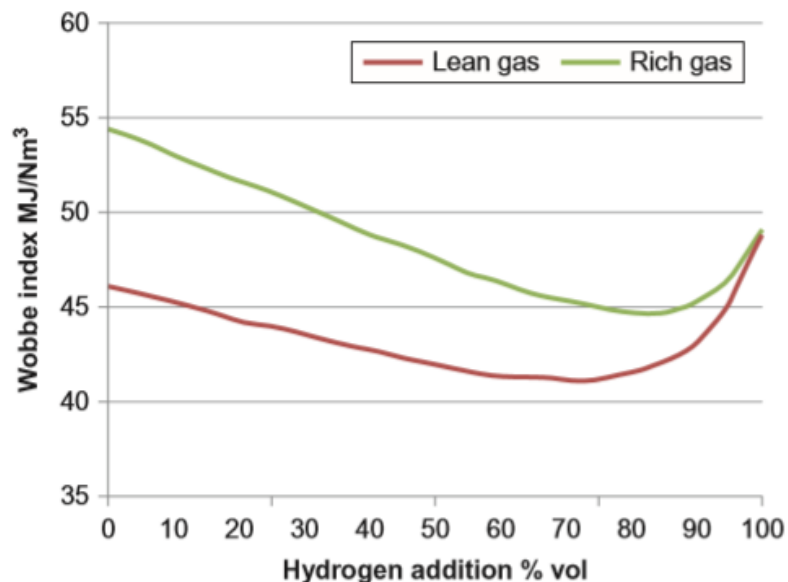


Figure 9: Wobbe-index behavior with different H₂-NG mixtures [39]

Therefore, a correct and appropriate choice for the transportation of the H₂-NG mixtures in the existing NG pipelines' network is the fundamental importance: currently, most conservative research utilizes a concentration of hydrogen of 10% vol. However, for the hydrogen-natural gas transportation, according to the adopted concentrations, the following infrastructure modifications have been considered [41].

| H2 INJECTION RATE | |
|-------------------|--|
| Under 5% | NO changes are needed for low pressure distribution pipelines and end-use appliances |
| 5-20% | Meters and detectors need to be changed in order to monitor gas columns and avoid gas leakages |
| 20-50% | Various changes are needed for meters and detectors, as well as end-use appliances |

Table 4: Infrastructure modifications according to the hydrogen injection rate

In this work has been analysed an injection rate of hydrogen under 5%: in particular, a H₂-NG mixture with a concentration of hydrogen of 2%vol has been considered due to the fact that, given the large geographic scope and scale of the existing natural gas infrastructure, even very low blend levels (less than 3%–5%) could absorb very large quantities of wind and/or solar power.

2.2 The Renewable potential of Algeria

Algeria plays a central role in energy world: it is a major producer and exporter of oil and natural gas, as previously discussed, but its geographic location has also several advantages for extensive use of most of renewable energy sources (RES), especially solar source.

Algeria is situated in the centre of North Africa, between the 38-35° of latitude north and 8-12° longitude east, has an area of 2 381 741 km² (the Sahara covers approximately the 86% of the total area of the whole Country) and a population of 32.5 millions of inhabitants (13.7 inhabitant/km²).



Figure 10: Algeria

The climate is transitional between maritime (north) and semiarid to arid (middle and south) and its average annual temperature is 12 °C. The Country has a great potential in solar energy with an average annual sunshine of 2000 h and with a solar power irradiation estimated of about 1700 kWh/m²/year, in the north, and of about 2650 kWh/ m²/year in the south [8].

In case of other renewable sources, the potential is more moderate, especially hydroelectricity and wind power when wind speeds are included between 2 and 6 m/s only, the potential of biomass⁹ is estimated at 1.33 Mtoe/year, while the geothermal energy has a more favourable outlook with 200 hot springs listed [9].

From the statistics of the “International Energy Agency” (IEA), between the 1990-2016, is possible to see (Fig. 11) how the electricity generation from renewable sources is anyway dominated by hydropower and only in 2014 the electricity from solar PV and wind started to grow.

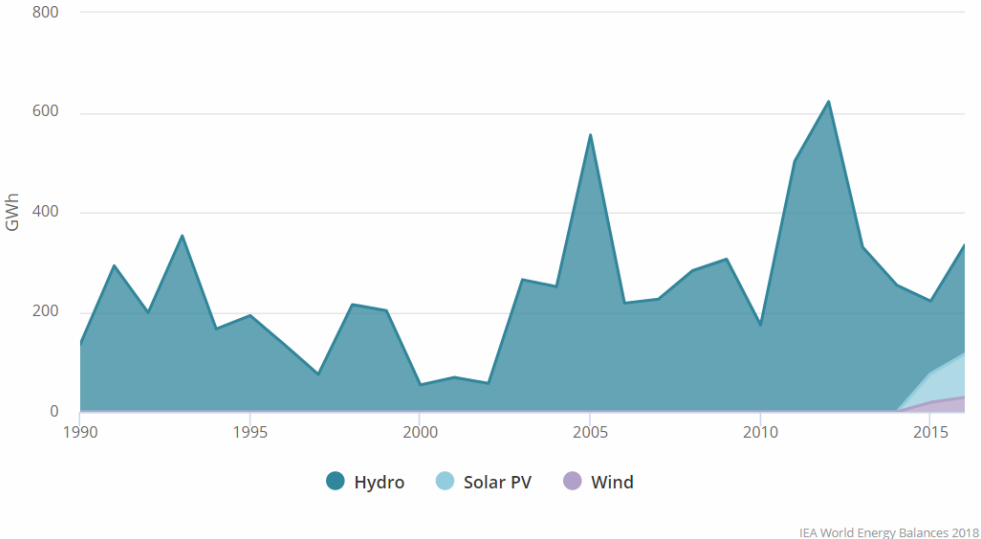


Figure 11: Electricity generation from renewable sources, Algeria (1990-2016) [1]

In order to diversify the electricity production ways and to preserve the fossil resources, the integration of renewable energies into the national energy mix constitutes one of the main objectives of the Algerian energy policy. In February 2011, in fact, the “National Program for the Development of Renewable Energy” (2011-2030) was adopted by the government.

This renewable energy program aims to use extended renewable sources, mainly photovoltaic systems and solar power and, to a lesser extent, wind power. It provides to install 22 GW (between 2011 and 2030) which represents 40% of whole energy consumption from renewable source by 2030.

⁹ The potential of biomass includes the recycling of waste from human activities, urban and agricultural waste.

The objectives of the new renewable energy program in Algeria are shown in **Fig. 12**: achieving this program will allow to reach by 2030 a part of renewable of about 27% in the national report of electric production [13].

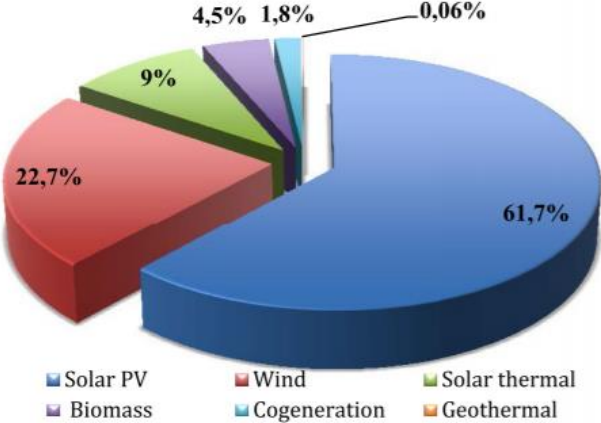


Figure 12: Objectives of renewable energy production program in Algeria by 2030 [12]

Among the different renewable energy sources exploitable in the Algerian territory, a particular attention, in this work, is given to solar and wind resources due to the nature of the designed hybrid plant (pv-wind-storage system). In the following table, is showed the distribution (in percentage) of installed power per resources, reported by the Algerian “Ministry of Energy and Mining” (MEM) [10].

| RESORCES | Installed Power [W] | % |
|--------------|---------------------|-----|
| SOLAR | 2 279 960 | 97 |
| WIND | 73 300 | 3 |
| TOTAL | 2 353 260 | 100 |

Table 5: Current distribution of installed power per resources [10]

As previously discussed, the solar energy potential of the Country is higher than the wind energy one and this explain the reason of the great difference in the installed power. In particular, the daily solar energy varies from a low average of 4.6 kWh/m² in the north to a mean value of 7.2 kWh/m² in the south.

In order to have an idea overall daily exposure [kWh/m²/day] received by Algeria, a solar distribution map is reported in **Fig. 13**.

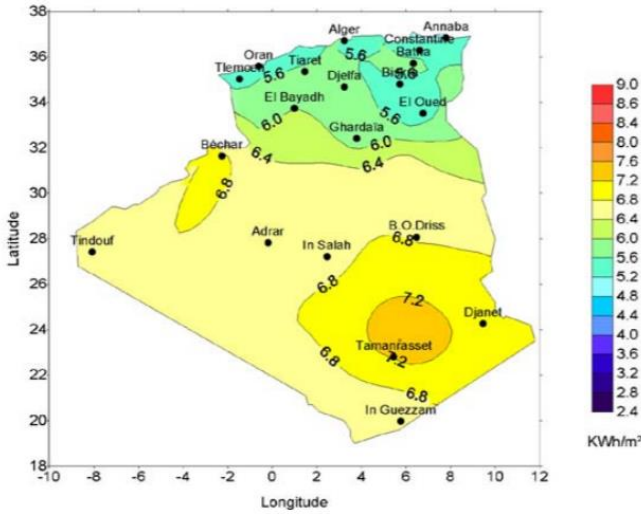


Figure 13: Overall daily average exposure received in Algeria [8]

From this map of “Renewable Energy Development Centre” (CDER), it seems that the South-East of Algeria is the best region for taking advantage of the solar energy potential [11], while in case of wind resource, studies always performed by the “Renewable Energy Development Centre” (CDER), during recent years, show that the climatic conditions in Algeria are also favourable for wind energy utilisation. The wind map (**Fig. 14**) established by the “Ministry of Energy and Mining” (MEM) shows that 50% of the Country surface presents a considerable average speed of the wind: the best wind energy potential is in the South, especially in the South-Western region where the average wind velocity is higher than 6 m/s.

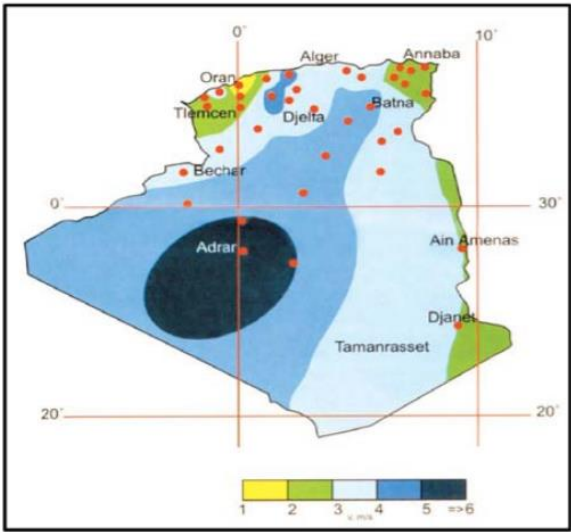


Figure 14: Wind chart of Algeria [8]

According to these studies, the best Algerian region for developing renewable projects, based on solar or wind-only sources, is the South of the Country. Nevertheless, in this study, the designed hybrid renewable plant has been placed in Hassi R'Mel, North-East of the Country, because of economic choices related to the transportation costs of the produced hydrogen: the three natural gas pipelines, in fact, are present in this geographical area. Furthermore, Hassi R'Mel (Province: Laghouat) is also characterized by excellent values of solar irradiance and wind speed and, in case of a combination of solar-wind resources (hybrid project), the Laghouat Province is an optimal option: this will be presented more in detail in the section 2.3 of the work.

2.3 Algerian hydrogen potential from renewable energy

The hydrogen has the potential to solve all major challenges related to the renewable energy transition of Algeria: for these reasons, its renewable production¹⁰ and its transportation is of great interest today. Many studies and research programs have been developed in order to find the best way to produce and transport this important carrier fluid. In particular, renewable hydrogen is mainly an economic option in Countries with a large renewable resource, as the Algeria.

In this study, has been taken into account only the electrolysis process for the hydrogen generation which consists in splitting the water molecule into its constituent elements (H₂ and O₂) using electricity. One advantage of water electrolysis is that compatible with a large variety of available renewable energy technologies, namely, solar, hydro, wind, wave, geothermal, etc.

Considering only solar and wind resources, a study about the Algerian potential in the hydrogen production, via electrolysis, has been conducted by two Universities of Algeria together with the Energy Department of Madrid¹¹. The analysis has been summarized in a scientific article: "*Prospects of hydrogen production potential from renewable resources in Algeria*", 2016, whose results have been reported (**Fig.15**) in this thesis study.

¹⁰ The renewable energies are a desired energy source for hydrogen production due their abundance, diversity and potential for sustainability.

¹¹ The Universities that have been conducted the analysis are: University of Ouargla 30000 (Algeria), University of Sidi Bel Abbes 22000 (Algeria) and the Department of Energy - Division of Renewable Energy of Madrid (Spain).

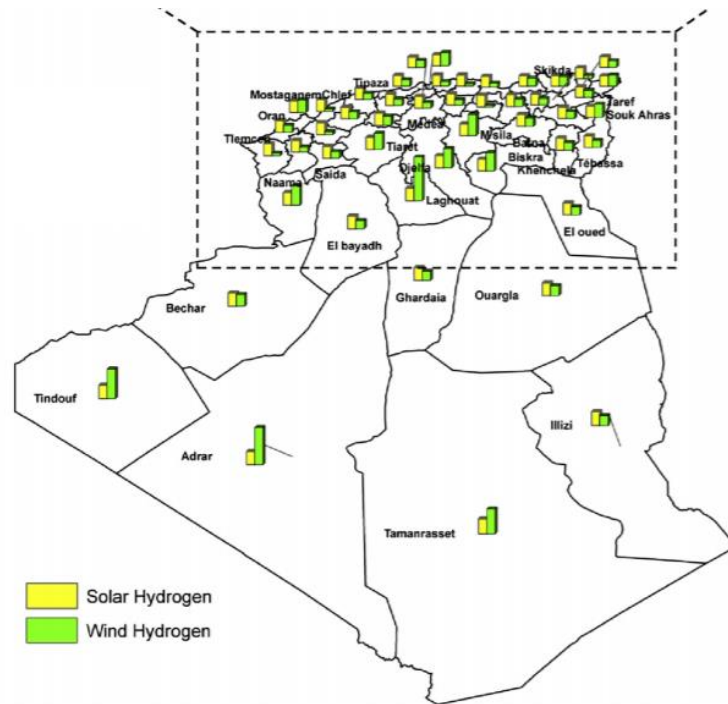


Figure 15: Comparison of solar and wind hydrogen production in Algeria [12]

These results are the fundamental interest for the case analysed in this work because, thanks to them, it's possible to indicate the optimal regions (in Algeria) for projects of hybrid solar-wind hydrogen production. From the map (**Fig.15**), it's evident that the distribution of hydrogen production from solar and wind behaves differently, and that is due to the varied nature of the source, the geographic site specification, climatic conditions, etc. In particular, the highest potential for producing solar photovoltaic hydrogen, in the whole Country, is located in South of Algeria (Tamenrasset), but it doesn't present important differences between the Algerian regions. On the contrary, the hydrogen produced from wind energy shows a remarkable different behaviour than the one observed for the solar and varies significantly by region. From the reported map, it's clear that the regions of Hassi R'Mel (Laghouat), Adrar and Tindouf present the highest potential for wind hydrogen production. Summing the hydrogen production potential for wind and solar energies, the Algerian optimal regions results: Adrar and Laghouat.

For these considerations (together with the considerations related to the hydrogen transport costs), the Algerian region chosen for the location of the hybrid plant has been the Laghouat region, in particular: Hassi R'Mel site. Moreover, an accurate analysis of the climatic conditions of the specific site has discussed, in this work, in the section 3 related to the "Case study".

2.4 Hassi R'Mel: Integrated Solar Combined Cycle (ISCC) power plant

Hassi R'Mel has a favourable geographical position for natural gas network and for exploitation of solar and wind resources. For these reasons, it has been the interest site of different energy projects as this Integrated Solar Combined Cycle (ISCC) power plant.

Near Hassi R'Mel, in fact, is already located an important ISCC power plant. The 150 MW Hassi R'Mel power plant (60 km from Ghardaia, in the northern central region of Algeria) is the first ISCC power system generating facility in the world¹². This project was promoted by Solar Power Plant One (SPP1), an Abener¹³ and NEAL ("New Energy ALgeria") joint venture formed for this purpose, which operates and exploits the plant for a period of 25 years.

The hybrid plant consists of two 40 MW gas turbines, one 80 MW steam turbine, and two parabolic trough solar fields with a total generating capacity of 25 MW. The solar fields comprise 224 parabolic collectors, in 56 loops, in an area measuring 180 000 m², with an inlet heat transfer fluid (HTF) temperature of 290 °C and an outlet temperature of 390 °C: the output from the solar array is used in the steam turbine. The annual power produced is expected to reach 1250 GWh/year [16].

The solar resource used in this hybrid project, allow a partial substitution of the fossil fuel (natural gas): in this way, it's possible to cut a part of CO₂ emissions normally generated in case of a traditional power station.



Figure 16: ISCC power plant of Hassi R'Mel

¹² The construction contract of the hybrid plant was signed on January 5, 2007, the hybrid plant was inaugurated July 14, 2011 and begun producing electricity in June 2011.

¹³ ABENER is a Spanish Company.

3. Technical feasibility of a hybrid system for the hydrogen production: Case study

This section mainly consists of two parts:

1. The geographic and meteorological characteristics of the selected site;
2. The design of each sub-system of the proposed hybrid plant together with the considered mathematical models;

Furthermore, in this study, the following general assumptions must be taken into account:

- a) The hydrogen generated by the plant is directly sent, together with the natural gas, in pipeline (with the 2%vol of hydrogen, choice previously discussed in the work);
- b) In the designed hybrid plant is not considered also a hydrogen storage-system;
- c) The electrical energy produced by the PV-WIND-STORAGE system is used exclusively by the electrolyzers for the production of hydrogen and, therefore, the whole system is not connected to the Algerian electrical grid.

3.1 Geographical and Meteorological Characteristics of the site

The site selected for the hybrid plant's project has been: **Hassi R'Mel (33.0120N/2.9878E, 731 m above the sea level)**, located in Laghouat (region of Algeria). This choice is due to the following factors:

- ✓ Its favourable geographical position for the natural gas network: it is located in proximity to inlets of three of the four export gas pipelines in North Africa. This constitutes an advantage in terms of transportation costs of the produced hydrogen;
- ✓ Its higher potential, together with the Algerian region of Adrar, for the hydrogen production by solar and wind resources (see section 2.3).



Figure 17: Hassi R'Mel (33.0120N/2.9878E) from Meteonorm 7.3 Software

Thanks to the Software *Meteonorm 7.3* it has been possible to obtain and evaluate the values related to the solar irradiation and wind speed of the selected location: for the output values, on *Meteonorm*, has been selected a “future scenario” (2020).

The solar irradiation and wind speed values computed on a monthly scale are of fundamental importance for the calculation of the potential energy productivity of the hybrid system.

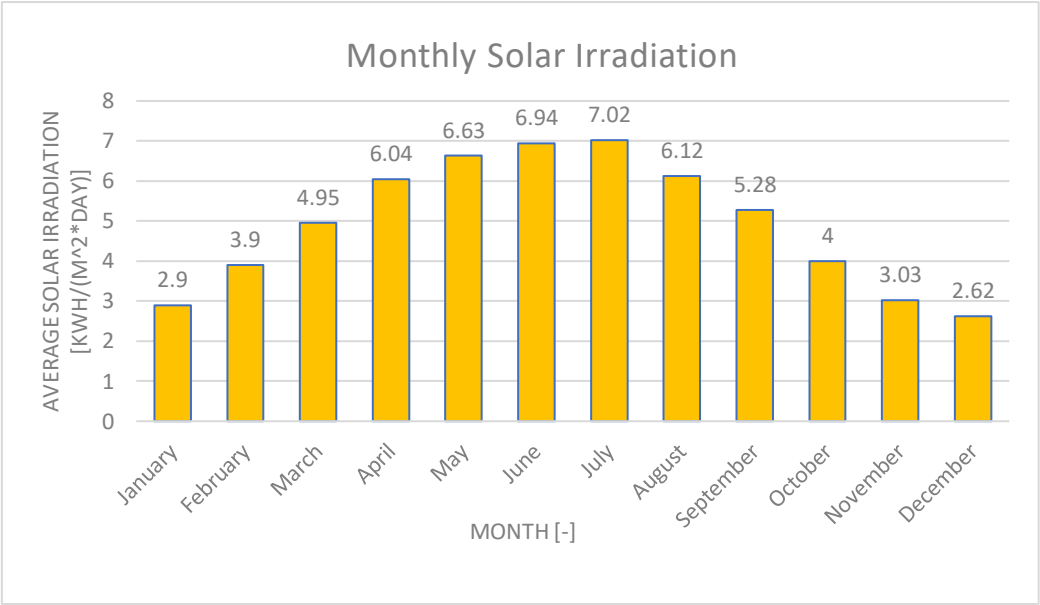


Figure 18: Monthly Solar Irradiation of the Site

From the graph, it’s possible to see that the maximum average solar irradiation, for the site, occurs in the month of July (7.02 kWh/m²/day), while the minimum value (2.62 kWh/m²/day) is present in the month of December. Obviously, the value of solar irradiation is higher during the summer months (June, July and August) reaching its peak in July, while the lower values are in correspondence of the winter months (December, January and February). For the chosen location, the annual average solar irradiation is 4.95 kWh/m²/day.

In case of wind speed, the anemometers from which the *Meteonorm Software* takes the data are located at a height of 10 meters. Monthly average wind speed values illustrated in the following chart are therefore referred to the same height.

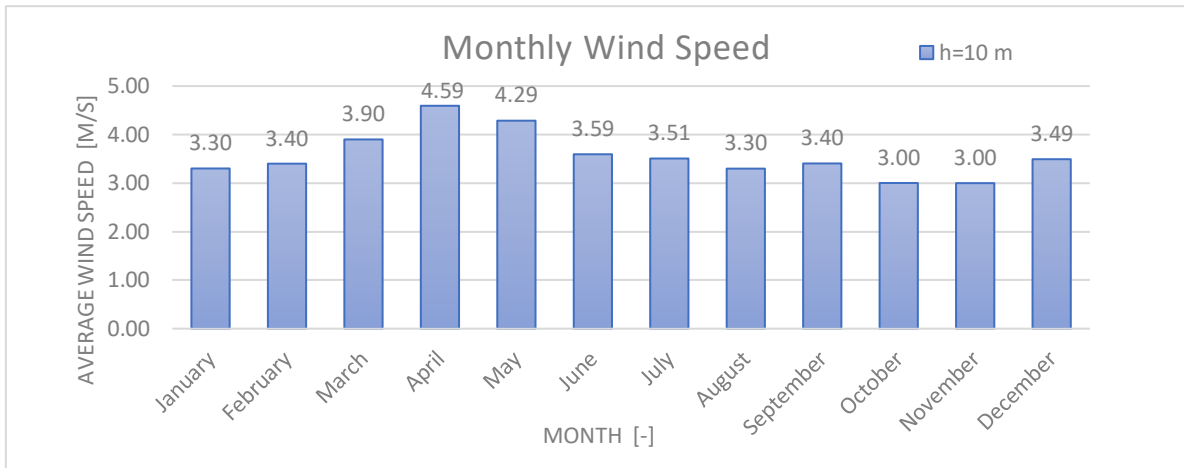


Figure 19: Monthly Wind Speed at height of 10 m

It is possible to see how the monthly wind speed distribution is more irregular than the solar irradiance. From the histogram, it can be noticed that the month characterized by the higher average wind speed is April (with an average wind speed of 4.59 m/s), while the minimum value is registered during the months of October and November (3.00 m/s). The annual average wind speed, for the selected location, is 3.56 m/s at a standard height of 10 m.

In order to have an idea of the number of hours in a year in which the wind speed is contained in a determinate interval (bin), the data obtained by *Meteonorm* (at 10 m) have been rearranged in bins of 1 m/s. In this way, a wind speed frequency distribution has been generated: the peak of hours (nearly 1800 hours) is registered for the bin of 2-3 m/s: this means that, during a year, for approximately 1800 hours, the wind speed is between 2 and 3 m/s at a standard height of 10 m.

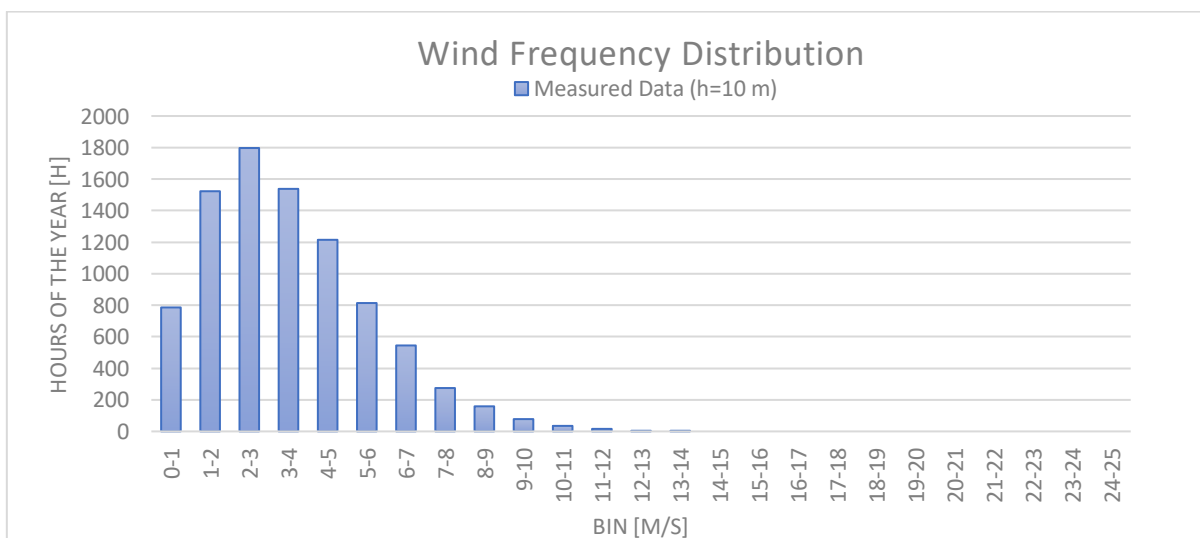


Figure 20: Wind Frequency Distribution at 10 m

It is important to notice that these wind speed values are referred to a relatively low height (10 m) and, with the increment of the height, also the average wind speed tends to increase: this consideration is necessary for the design of the wind system.

3.2 Design of the hybrid plant's sub-systems: Mathematical Models

In this section, all the assumptions, considerations and mathematical models used for the design of the PV-WIND-STORAGE system for the hydrogen production are exposed. The load demand of the PEM electrolyzers' system is analysed in the last part of this section.

To follow, a simplified sketch of the whole studied system is showed.

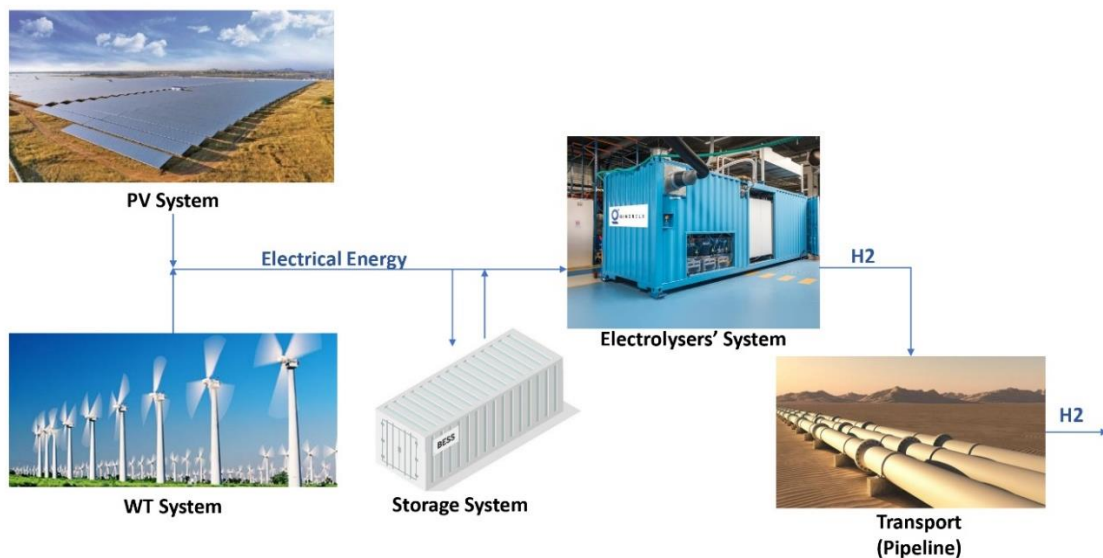


Figure 21: Scheme of the Hybrid System

It's important to point out that this study does not take into account some technical factors related to the PV-WIND-STORAGE system, as:

- ✓ The configuration of the wind turbines (WTs)¹⁴, PV panels and batteries into the wind farm, PV and storage system, respectively;
- ✓ The “wake effect” generated by the upwind turbines and “shading effect” produced by the PV array: phenomena that tend to reduce the productivity of the considered systems and would be necessary to analyse in a complete design study;
- ✓ The electrical and power electronics devices normally present in a PV and wind system.

¹⁴ It has been considered, for the WTs, only an average distance factor equals to 8.

3.2.1. Wind System

In order to calculate the possible energy productivity of a wind system, in a specific location, it is firstly necessary to study the energy output of a single wind turbine (WT). The energy productivity of a WT is function of:

- ✓ The manufacturer characteristic (power) curve of the WT;
- ✓ The wind speed to the hub height.

For this study, has been considered a Horizontal Axis Wind Turbine (HAWT) of 3 MW whose technical specifications are displayed in **Table 6**, while its power curve is shown in **Figure 23**. The choice to select an HAWT is given to the fact that they are more efficient than the Vertical Axis Wind Turbines (VAWTs). In particular, among the different HAWTs, the most efficient WTs are the 3-blade rotor with lower Tip Speed Ratio (TSR¹⁵ between 5-10), as it is possible to see from the **Figure 22**.

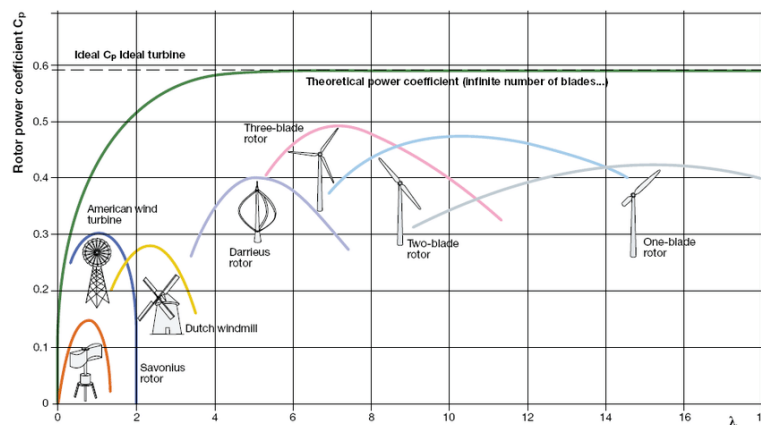


Figure 22: Cp vs. TSR of WTs [18]

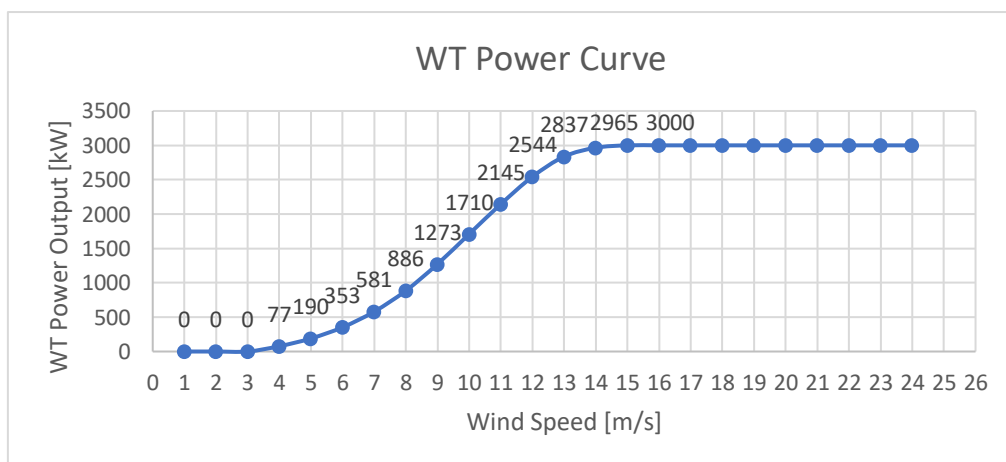


Figure 23: Manufacturer characteristic (Power) Curve of the selected WT [17]

¹⁵ The Tip Speed Ratio (TSR) of a WT is the ratio between the wind turbine speed and the wind speed.

| TECHNICAL DATA | 1 WT (Vestas V90-3.0) |
|-------------------------------------|------------------------|
| Type | Horizontal Axis (HAWT) |
| Number of blades [-] | 3 |
| Blades tangential speed [m/s] | 75.87 |
| Blades angular speed [rad/s] | 1.69 |
| Rotor rated speed [rpm] | 16.1 |
| Rated Power [MW] | 3 |
| Rotor Diameter [m] | 90 |
| Swept Area [m ²] | 6362 |
| Blades length [m] | 45 |
| Hub height [m] | 105 |
| Occupied Area [km ²] | 0.45 |
| Power density [MW/km ²] | 6.68 |
| Wind Class | IEC IIA/IIIA |
| Standard Temperature range [°C] | from -20 to 40 |
| Cut-in speed [m/s] | 4 |
| Nominal speed [m/s] | 15 |
| Cut-out speed [m/s] | 25 |

Table 6: Technical Data of the selected WT [17]

The Wind Turbine (WT) is a device which converts the kinetic energy of the wind into rotational energy (mechanical energy): it is coupled with an electrical generator which generates electricity and so there is an indirect conversion from mechanical to electrical energy.

The WT's power curve, during a productivity analysis, is the fundamental importance because it is able to give information about the power output of the WT for each value of the wind speed. The power output of a wind turbine (P_{WT}), in fact, is a function of the power coefficient (C_p)¹⁶, air density (ρ_{air})¹⁷, swept Area (A_{swept}) and wind velocity (v_{wind}), according to the following cubic "law":

(1)

$$P_{WT} = \frac{1}{2} \cdot C_p \cdot \rho_{air} \cdot A_{swept} \cdot v_{wind}^3$$

In case of a wind speed lower than the *cut-in* speed (for this WT equals to 4 m/s) or higher than the *cut-out* speed (for this WT equals to 25 m/s), the WT's power output is equal to zero, while the WT's rated power (in this case 3 MW) is reached with a wind speed between the *rated wind speed* ($v_R = 15$ m/s) and the *cut-out* speed. The following "mathematical model" clearly explains this situation:

¹⁶ The maximum power coefficient, C_p , is 0.59 (Betz limit): it represents the efficiency limit from wind kinetic to mechanical energy.

¹⁷ The value of air density used for calculating the energy productivity of the WT is equal to 1.225 kg/m³ (T=15°C above sea level).

$$P_{WT} = \begin{cases} 0 & \text{if } v_{wind} < v_{cut-in} \text{ or } v_{wind} > v_{cut-out} \\ \frac{1}{2} \cdot C_p \cdot \rho_{air} \cdot A_{swept} \cdot v_{wind}^3 & \text{if } v_{cut-in} < v_{wind} < v_R \\ P_{RATED} & \text{if } v_R \leq v_{wind} < v_{cut-out} \end{cases}$$

Since wind speed data reported in this study and extrapolated from *Meteonorm* are obtained at a height of 10 m and the selected WT has a hub height of 105 m (see **Table 6**), the measured wind speed must be “adjusted” to the wind turbine hub height due to the increment of wind speed with the height. For this goal, has been applied the Hellman exponential law, as shown in the following equation [21]:

$$\frac{v}{v_0} = \left(\frac{h}{h_0}\right)^\alpha \quad (2)$$

Where

h : is the desired height equals to 105 m, [m];

h_0 : is the reference height equals to 10 m, [m];

v : is the annual average wind speed at the desired height (h), [m/s];

v_0 : is the annual average wind speed measured at the reference height (h_0), [m/s];

α : is the surface roughness coefficient which gives information about the ground’s nature and the possible presence of obstacles on the analysed surface area, [-].

In most studies, the surface roughness coefficient is assumed to be 0.143 (1/7), but it can also be determined from the following expression [19]:

$$\alpha = \frac{[0.37 - 0.088 \cdot \ln(v_0)]}{[1 - 0.088 \cdot \ln\left(\frac{h_0}{10}\right)]} \quad (3)$$

This approach is used in this study¹⁸. A summary of these values is reported in the following table together with the obtained values for the annual average wind speed at the required height (v) and for the surface roughness coefficient (α).

¹⁸ This formula has been applied for a study about the power generation of a wind farm in the region of Adrar (Southern Algeria) [19] and has also been utilized in this work due to the similar meteorological conditions of two Algerian regions in terms of hydrogen production by wind and solar resources.

| | |
|----------------------------|-------|
| h [m] | 105 |
| h_o [m] | 10 |
| v [m/s] | 6.54 |
| v_o [m/s] | 3.56 |
| α [-] | 0.258 |

Table 7: Obtained values because of the wind speed variations with height

After calculating the surface roughness coefficient, the monthly average wind speed values referred to the hub height have also been obtained utilizing always the power law reported in the equation (2) and taking as reference the values for standard height (10 m).

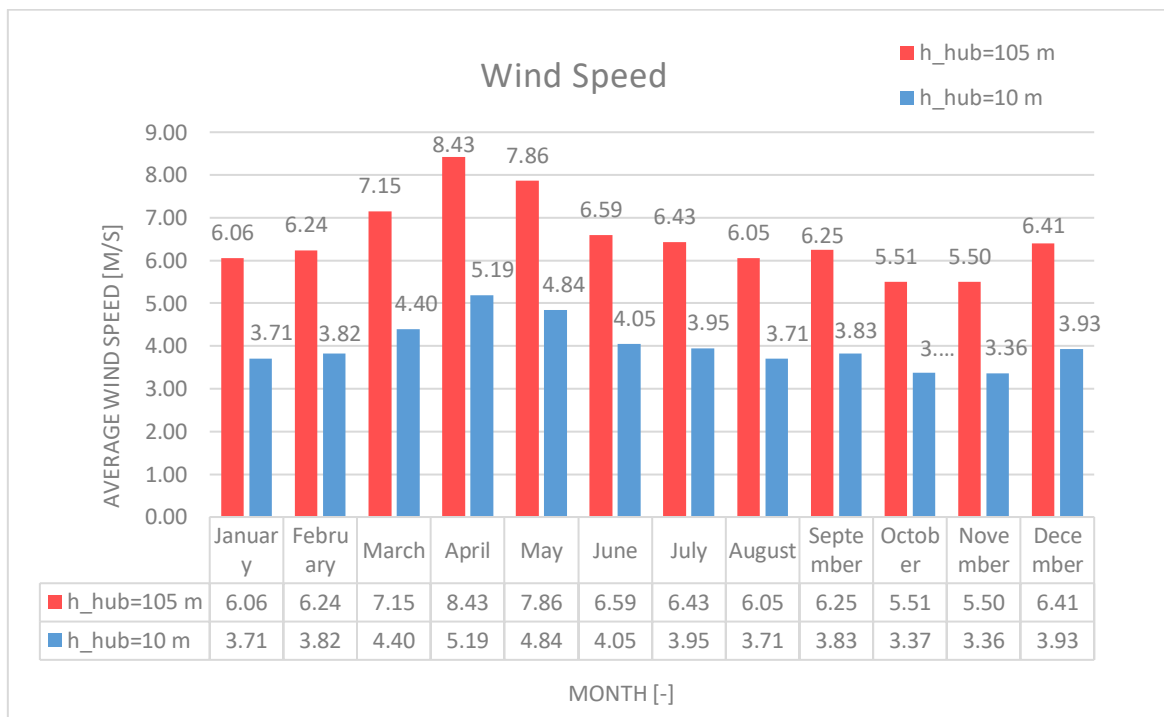


Figure 24: Monthly Wind Speed at hub height (105 m) vs. Monthly Wind Speed at reference height (10 m)

As previously discussed, the increment of the height produces also an increment in the wind speed: at a great distance from the ground, the effect of this becomes negligible and the wind speed is only function of meteorological conditions [20].

Before proceeding with the description of the model used in this work, it is important to point out that a detailed wind speed profile, which is the base for a correct WT energy productivity study, requires knowledge of both wind speed and wind direction. The wind direction is not considered in this study because of the limited information about this aspect, while the information obtained for the wind speed are only related to the reference height of 10 m. In

particular, from *Meteonorm*, it has only been possible to obtain the wind speed values for each hour of the year while, a correct analysis, includes wind speed values every 10 minutes and for different heights.

For these reasons, in order to estimate the annual energy productivity of the WT, two different techniques for the calculation of the wind distribution at hub height have been adopted:

- 1) WIND DISTRIBUTION FROM MEASURED DATA;
- 2) WEIBULL PROBABILITY DENSITY FUNCTION.

3.2.1.1 Wind distribution from measured data

With this technique, the hourly wind speed referred to the hub height has been calculated adjusting, for each hour of the year, the hourly wind speed obtained by *Meteonorm* (at 10 m) with the power law (equation (2)) and considering the surface roughness coefficient (α) previously computed. Moreover, thanks to the power curve of the WT, the annual energy production can be expressed as follow:

$$E_{WT} = \sum_{i=1}^n P_{WT,i} \cdot t \quad [MWh] \quad (4)$$

Where

E_{WT} : is the annual energy production of the WT, [MWh];

n : is the number of hours in a year. The year, in this study, is a leap year (2020) because on *Meteonorm* has been chosen a “*future scenario*”, so $n = 8784$ [-];

$P_{WT,i}$: is the hourly Wind Turbine (WT) power output based on its power curve according to the wind speed registered for each hour, [MW];

t : is one-hour time duration, $t = 1h$ [h].

The trend of the energy produced by the WT, for each hour of the year and in the selected location, has been showed in the following figure.

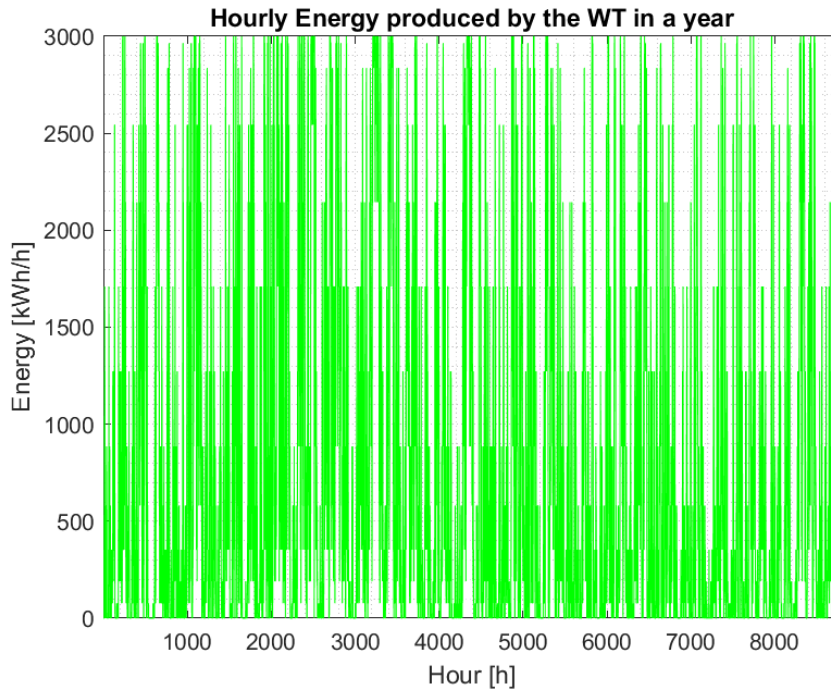


Figure 25: Hourly Energy produced by the WT in a year

It's possible to see (Fig. 26) how the energy generated by the wind turbine is higher in the month of April and lower in the months of October and November due to the monthly wind speed registered in these months: the higher and lower, respectively (see Fig. 24).

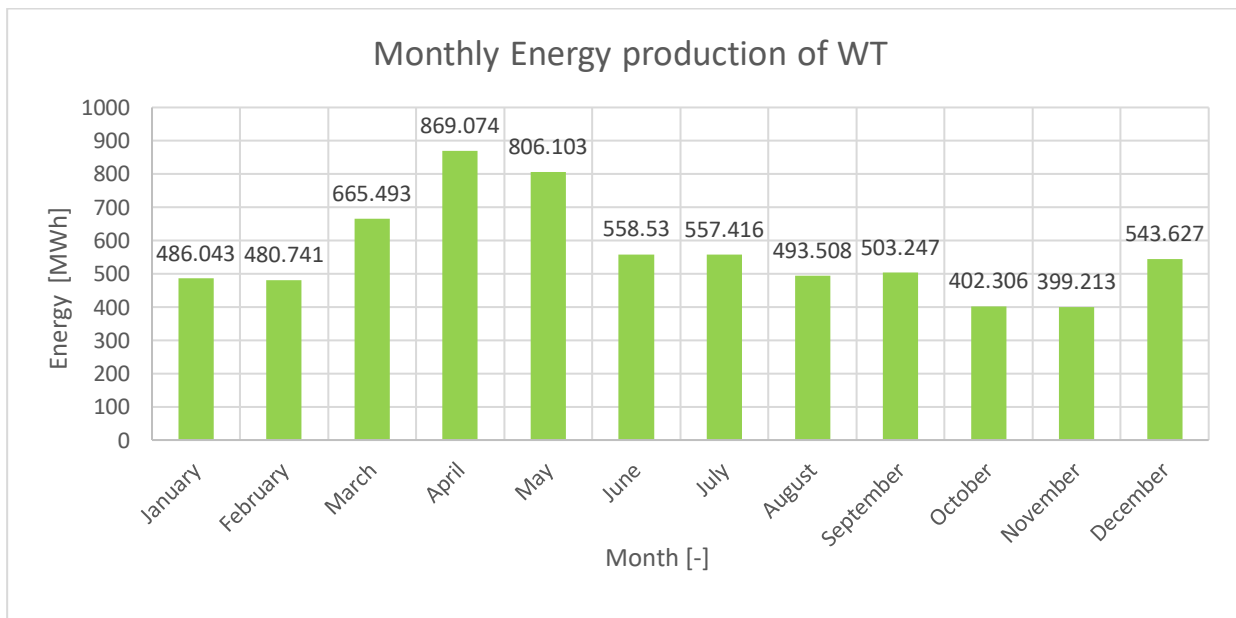


Figure 26: Monthly Energy production of WT

The result obtained with this approach, in terms of total annual energy produced by the WT, according to the equation (4), is:

| E_{WT} [MWh] | C_f ¹⁹ [%] | h_{eq} ²⁰ [h] |
|----------------|-------------------------|----------------------------|
| 6765.30 | 25.7 | 2255 |

Table 8: Annual energy produced by the WT, WT's Capacity factor (C_f) and WT's equivalent hours (h_{eq})

3.2.1.2 Weibull Probability density function

With this technique it is possible to obtain the wind speed frequency distribution at hub height and, among the different probability density functions, the Weibull distribution technique is widely accepted and used in order to estimate a site's probability distribution of wind speeds. The Weibull probability function, in fact, usually provides the best fit of measured wind data [20].

This density function is expressed by:

$$f_w(v) = \left(\frac{k}{c}\right) \cdot \left(\frac{v}{c}\right)^{k-1} \cdot \exp\left[-\left(\frac{v}{c}\right)^k\right] \quad (5)$$

Where

$f_w(v)$: is the wind probability density function;

v : is the wind speed, [m/s];

k : is the Weibull shape parameter which is a measurement of the width of distribution²¹, [-];

c : is the Weibull scale parameter which is closely related to the mean wind speed, [m/s].

¹⁹The capacity factor, C_f , is one of the most important indicators for assessing the field performance of a wind turbine. It is defined as the ratio of the energy actually produced by the system to the energy that could have been produced, if the system operated at its rated power throughout the time period. In this case, the C_f has referred to a time period of a year:2020 (leap year: 8784 h).

²⁰ The equivalent hours, h_{eq} , are the operational hours of the wind turbine at the rated power.

²¹ $k=2$ is a special case of the Weibull distribution called the Rayleigh distribution. In general, with a value of k close to 1, the Weibull distribution is more irregular, while in case of values of k comprise between 2-3, the Weibull distribution is more symmetrical (similar to the Gaussian distribution).

With the Weibull probability density function is possible to obtain the extrapolated values of wind speed at different heights. The Weibull parameters at the desired hub height, k_{hub} and c_{hub} , are obtained using the following relations:

$$k_{hub} = k_0 \cdot \frac{[1 - 0.088 \cdot \ln\left(\frac{h_0}{10}\right)]}{[1 - 0.088 \cdot \ln\left(\frac{h}{10}\right)]} \quad (6)$$

$$\frac{c_{hub}}{c_0} = \left(\frac{h}{h_0}\right)^m \quad (7)$$

Where

k_0 : is the Weibull shape parameter at the measurement height, [-];

c_0 : is the Weibull scale parameter at the measurement height, [m/s];

k_{hub} : is the Weibull shape parameter at the desired height, [-];

c_{hub} : is the Weibull scale parameter at the desired height, [m/s];

h_0 : is the measurement height (10 m), [m];

h : is the desired height (105 m), [m];

while the exponent “m” is defined as:

$$m = \frac{[0.37 - 0.088 \cdot \ln(c_0)]}{[1 - 0.088 \cdot \ln\left(\frac{h_0}{10}\right)]} \quad (8)$$

The Weibull shape (k_0) and scale (c_0) parameters at the measurement height have been obtained taking into consideration the relations used by *Meteonorm* in case of tropical and subtropical climatic zones (with latitude comprises between 35°S and 35°N) [32]. Obviously, due to the variation of these parameters with the wind speed, in the equations (6), (7) and (8), have been considered their annual average values.

All these values are showed in the following table.

| | WEIBULL PARAMETERS | HEIGHT [m] |
|-----------------|-----------------------|------------|
| k_0 [-] | 1.84 | 10 |
| c_0 [m/s] | 4.01 | 10 |
| k_{hub} [-] | 2.32 | 105 |
| c_{hub} [m/s] | 7.18 | 105 |
| m [-] | 0.248 | - |

Table 9: Weibull's annual average parameters

In order to compute the Weibull probability density function, in the equation (5), the shape (k) and scale (c) parameters have been replaced with their values obtained for the desired hub height (k_{hub} and c_{hub}), while the wind speed values (v) have been varied from 1 m/s to 25 m/s: the *cut-in* and *cut-out* speed of the selected WT. In this way, it's possible to obtain the frequency distribution of the wind speed at the hub height ($f_w(v)$) that represents the percentage (or fraction) of occurrence of a specific wind speed, for the analysed hub height and for the considered year.

Thanks to the obtained wind distribution, the annual energy produced by the WT (for the selected site) can be achieved in the following way:

$$E_{WT} = \sum_{v=1 \text{ m/s}}^{25 \text{ m/s}} P_{WT,v} \cdot f_w(v) \cdot n \quad [MWh/y] \quad (9)$$

Where

E_{WT} : is the annual energy production of the WT, [MWh/y];

$P_{WT,v}$: is the hourly Wind Turbine (WT) power output based on its power curve according to the wind speed, [MW];

$f_w(v)$: is the wind probability density function which represents the fraction of occurrence of a specific wind speed, for the analysed hub height;

n : is the number of hours in a year. The year, in this study, is a leap year (2020) because on Meteororm has been chosen a "future scenario", so $n = 8784$ [-].

The following figures represent the results obtained from the Weibull distribution technique.

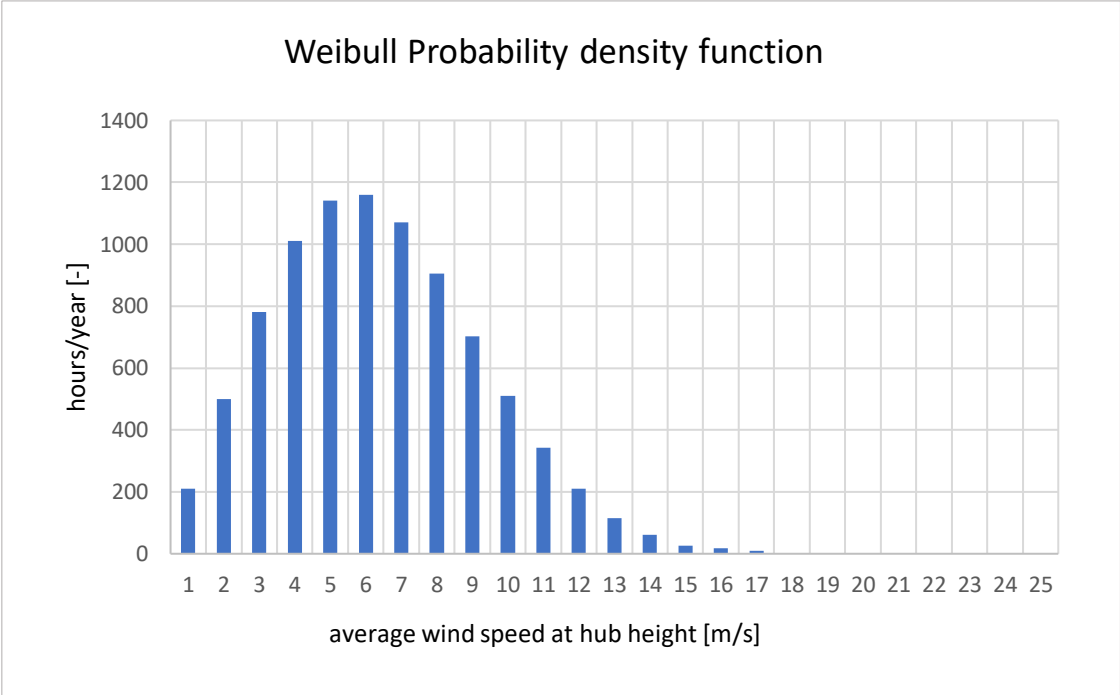


Figure 27: Weibull probability density function in terms of hours per year

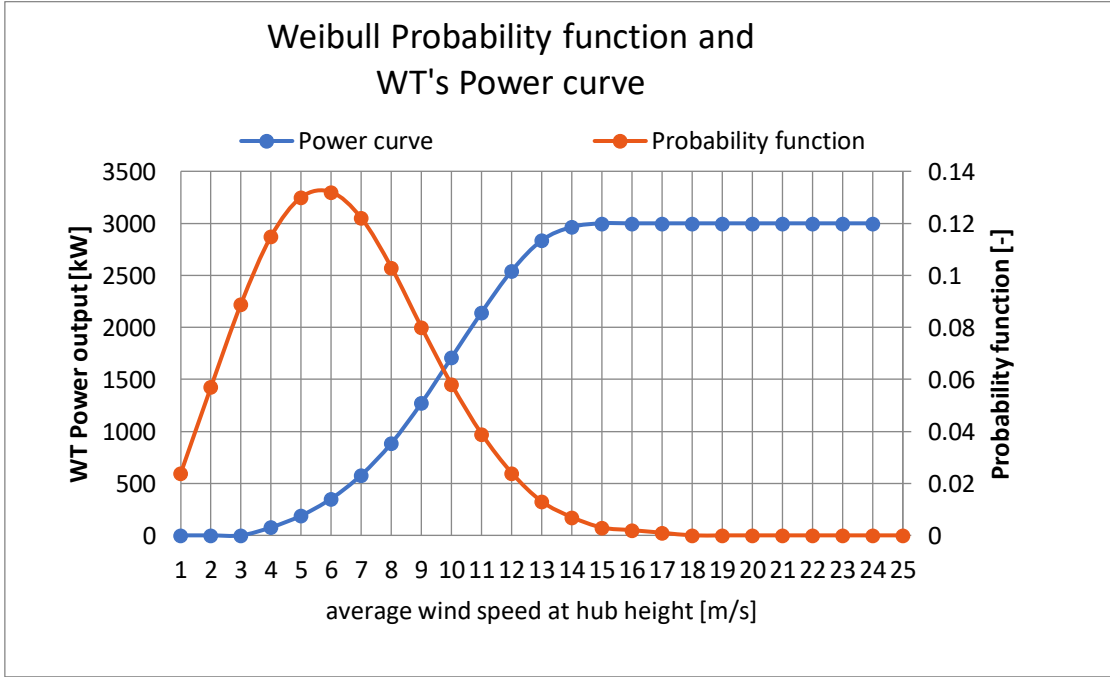


Figure 28: Weibull probability function and WT's Power curve

In the following table are showed all the necessary values for the calculation of the total annual energy production of the WT.

| v_{hub} [m/s] | $f_w(v)$ | WT's Power [kW] | Hours per Year [h/y] | Energy produced by the WT [MWh/year] |
|---------------------------|--------------|--------------------|----------------------------|--|
| 1 | 0.024 | 0 | 211 | 0 |
| 2 | 0.057 | 0 | 501 | 0 |
| 3 | 0.089 | 0 | 782 | 0 |
| 4 (cut-in speed) | 0.115 | 77 | 1010 | 77.782 |
| 5 | 0.130 | 190 | 1142 | 216.965 |
| 6 | 0.132 | 353 | 1155 | 409.299 |
| 7 | 0.122 | 581 | 1072 | 622.627 |
| 8 | 0.103 | 886 | 905 | 801.610 |
| 9 | 0.080 | 1273 | 703 | 894.563 |
| 10 | 0.058 | 1710 | 509 | 871.197 |
| 11 | 0.039 | 2145 | 343 | 734.826 |
| 12 | 0.024 | 2544 | 211 | 536.316 |
| 13 | 0.013 | 2837 | 114 | 323.963 |
| 14 | 0.007 | 2965 | 61 | 182.312 |
| 15 (rated speed) | 0.003 | 3000 | 26 | 79.056 |
| 16 | 0.002 | 3000 | 18 | 52.704 |
| 17 | 0.001 | 3000 | 9 | 26.352 |
| 18 | 0.000 | 3000 | 0 | 0.000 |
| 19 | 0.000 | 3000 | 0 | 0.000 |
| 20 | 0.000 | 3000 | 0 | 0.000 |
| 21 | 0.000 | 3000 | 0 | 0.000 |
| 22 | 0.000 | 3000 | 0 | 0.000 |
| 23 | 0.000 | 3000 | 0 | 0.000 |
| 24 | 0.000 | 3000 | 0 | 0.000 |
| 25 (cut-out speed) | 0.000 | 0 | 0 | 0.000 |

Table 10: Values for the calculation of the WT energy production

In **Table 10** are highlighted (in yellow) the wind speed values, at the hub height, that occur for more hours in the analysed year. The result obtained with this approach, in terms of total annual energy produced by the WT, according to the equation (9), is:

| E_{WT} [MWh] | C_f^{22} [%] | h_{eq} [h] |
|----------------|----------------|--------------|
| 5829.57 | 22.1 | 1943 |

Table 11: Annual energy produced by the WT, WT's Capacity factor (C_f) and WT's equivalent hours (h_{eq})

²²In this case, the C_f has referred to a time period of a year:2020 (leap year: 8784 h).

3.2.1.3 Comparison between the two approaches

For the calculation of the annual energy produced by the analysed WT, the two exposed techniques present differences in the obtained results.

| | E_{WT} [MWh] | C_f [%] | h_{eq} [h] |
|--|-------------------|--------------|-----------------|
| 1) Wind distribution from measured data | 6765.30 | 25.7 | 2255 |
| 2) Weibull distribution | 5829.57 | 22.1 | 1943 |
| Relative Error: 13.8% | | | |

Table 12: Comparison between the two approaches

In particular, with the Weibull distribution technique, the annual energy production of the WT (E_{WT}) is lower respect to that obtained with the first approach and, of course, this also occurs for the values related to the capacity factor (C_f) and equivalent hours (h_{eq}) of the WT. Between the results of two approaches, there is a relative error of 13.8%. This could be due to the considered wind speed range for the Weibull distribution: the smaller is the considered wind speed range and more accurate is the result.

It's important to note that the calculation of the WT's annual productivity has been obtained, with both the methods, only considering the integer values of the registered wind speed and, in case of a wind speed comprises between two points (is the case of the 1st approach), an approximation to the nearest integer has been adopted.

This is a simplified approach, but a more detailed and precise analysis includes an approximation method based on the interpolation of data provided by the manufactures in order to consider all the wind speed values [19].

In this feasibility study, to proceed with the design of the whole hybrid system, has been considered the annual energy production of the WT obtained with the 1st approach: in this way, has been possible to have the hourly energy output of the selected WT for the entire period of time.

3.2.2 PV System

The energy output of a single PV panel has been computed thanks to the help of a *PV-GIS Software* (“*Photovoltaic Geographical Information Software*”) selecting the Latitude and Longitude coordinates of the analysed location and considering a crystalline silicon (c-Si) PV technology. As solar radiation database has been selected the “*PV-GIS SARA*H” and has been considered the annual energy output of 0.3 kW of installed peak²³ PV power: in this way, it has been possible to evaluate the energy productivity of 0.3 kW of installed PV panel in the analysed site. The system loss has been set equal to 10%, while the tilt and azimuth angles of the PV panel have been found thanks to an option of the PV-GIS Software (“*Optimize slope and azimuth*”).

A view of the Software operational window, with the selected values, is shown below.

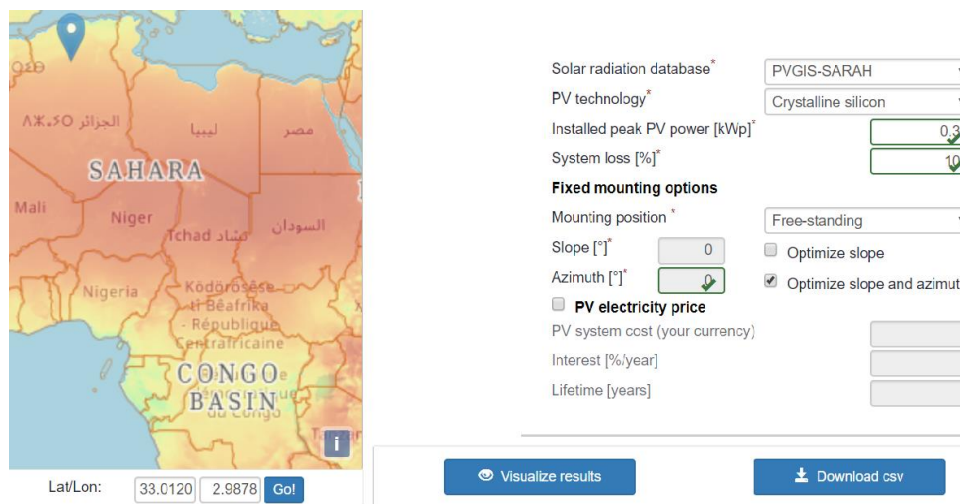


Figure 29: View of the PV-GIS Software operational window

while the results obtained by the Software have been reported in the following table.

| | |
|--|------|
| Tilt angle [°] | 33 |
| Azimuth angle [°] | -3 |
| Yearly PV energy production [kWh] | 598 |
| Yearly in-plane irradiation [kWh/m²] | 2430 |

Table 13: Results obtained by PV-GIS for 0.3 kW of installed peak PV power

²³ The peak power or nominal power is the power measured at Standard Test Conditions (STC). The STC are: irradiance of 1000 W/m² and PV module's temperature of 25 °C.

Thanks to the obtained annual energy production of a PV panel (with a peak power of 0.3 kW), it has also been possible to estimate the capacity factor (C_f) and the equivalent hours (h_{eq}) of the PV panel, in the selected site: 22.7% and 1993h, respectively.

The energy output of a PV system is function, of course, of the amount of solar radiation that arrives on the PV panels, but there are also other important factors affecting the energy output of PV system and they are considered in the calculation of *PV-GIS Software*²⁴, as:

- Irradiance and module's temperature;
- System losses and degradation with age;
- Effect of changes in the solar spectrum;
- Shallow-angle reflection.

In this section, it has been analysed and reported only the mathematical model used by the *PV-GIS* for taking into account the first effect related to the irradiance and PV module's temperature. For the other mathematical models (used by *PV-GIS*) that permit to consider the all mentioned effects that influence the performance of the PV panels, it's appropriate to make reference to the *PV-GIS*'s documentation [22].

The efficiency of PV panels depends on the temperature of the panel and on the solar irradiance. Generally, the efficiency decreases with increasing temperature²⁵ and, for most types of PV panels, the efficiency is nearly constant for solar irradiances from about 400 W/m² to at least 1000W/m² (for constant module temperature), but at lower irradiance the efficiency tends to decrease. For these reasons, for most places, the average module efficiency is a bit lower than the efficiency measured at the Standard Test Conditions²⁶.

PV-GIS Software calculates the effects of solar irradiance and PV module's temperature using a mathematical model²⁷ that assumes the power's dependence on solar irradiance, G , and PV module's temperature, T_m , in the following way:

$$P = G' \cdot A \cdot \eta_{nom} \cdot \eta_{rel}(G, T_m) \quad (10)$$

$$\begin{aligned} \eta_{rel}(G', T'_m) = 1 + k_1 \cdot \ln(G') + k_2 \cdot \ln(G')^2 + k_3 \cdot T'_m + k_4 \cdot T'_m \cdot \ln(G') + \\ + k_5 \cdot T'_m \cdot \ln(G')^2 + k_6 \cdot T'^2_m \end{aligned} \quad (11)$$

²⁴ The other effects that influence the energy output of a PV system, but not considered in *PV-GIS Software*, are: snow, dust and dirt and partial shadowing of the PV modules.

²⁵ This "phenomena" is also function of the PV technology.

²⁶ The Standard Test Conditions (STC) are: a solar irradiance of 1000 W/m² (G_{STC}) and a PV module's temperature of 25 °C (T_{STC}).

²⁷ The mathematical model used by *PV-GIS Software* has been described by Huld et al. 2011, "A power-rating model for crystalline silicon PV modules" [23].

Where

P : is the power output of the PV panel;

G' : is the normalized in-plane irradiance, defined as $G' = \frac{G}{G_{STC}}$;

A : is the frontal area of the PV panel;

η_{nom} : is the nominal efficiency of the PV panel;

η_{rel} : is the ratio of the module efficiency under given conditions of G and T to the efficiency at STC;

T'_m : is the PV module's temperature defined as $T'_m = T_{mod} - T_{STC}$;

The coefficients k_1 to k_6 are found for each PV technology by fitting to measured data. The coefficients used in *PV-GIS* are based on measurements performed at ESTI²⁸ [22].

In this work, has been selected a PV module with a nominal power of 0.3 kW whose technical characteristics have been reported in the following table.

| TECHNICAL DATA | 1 PV PANEL (TSM-PD14) |
|--|-----------------------|
| Material of Solar cells | c-Si |
| Solar cells' size [mm] | 156x156 |
| Number of Solar cells per PV module [-] | 72 (6x12) |
| PV module's size [mm] | 1956x992x40 |
| PV module's area [m ²] | 1.940 |
| Operational Temperatures [°C] | From -40 to 85 |
| STC – "STANDARD TEST CONDITIONS" ($G=1000 \text{ W/m}^2$, $T_{mod}=25^\circ\text{C}$) | |
| Nominal Power [W] | 300 |
| U_{mpp}^{29} [V] | 36.2 |
| I_{mpp}^{30} [A] | 8.28 |
| U_{oc}^{31} [V] | 45.4 |
| I_{sc}^{32} [A] | 8.77 |
| Efficiency, η [%] | 15.5 |
| NOCT – "NOMINAL OPERATING CELL TEMPERATURE" ($G=800 \text{ W/m}^2$, $T_{mod}=20^\circ\text{C}$) | |
| NOCT [°C] | 44 |

Table 14: Technical Data of the selected PV panel [24]

²⁸ ESTI is the "European Solar Test Installation" of the Joint Research Centre.

²⁹ U_{mpp} ("Maximum Power Point Voltage").

³⁰ I_{mpp} ("Maximum Power Point Current").

³¹ U_{oc} ("Open Circuit Voltage").

³² I_{sc} ("Short Circuit Current").

In the following figures are showed the trend of the energy production of the selected PV module for each hour of the year and in the considered location and, moreover, its monthly energy productivity. It's possible to see, from both the figures, that the energy production of PV panel is more stable if compared to that of WT (see **Fig.25-26**), but the energy productivity of WT is much bigger than that of PV module. This aspect, of course, will influence the sizing and the optimization analysis of the hybrid PV-WIND-STORAGE system: later developed in the work.

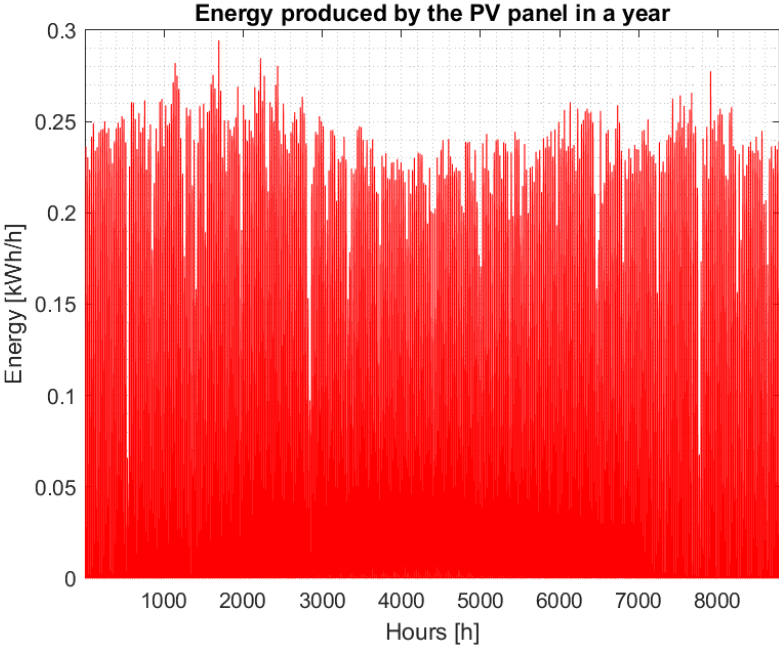


Figure 30: Hourly Energy Production of the PV panel

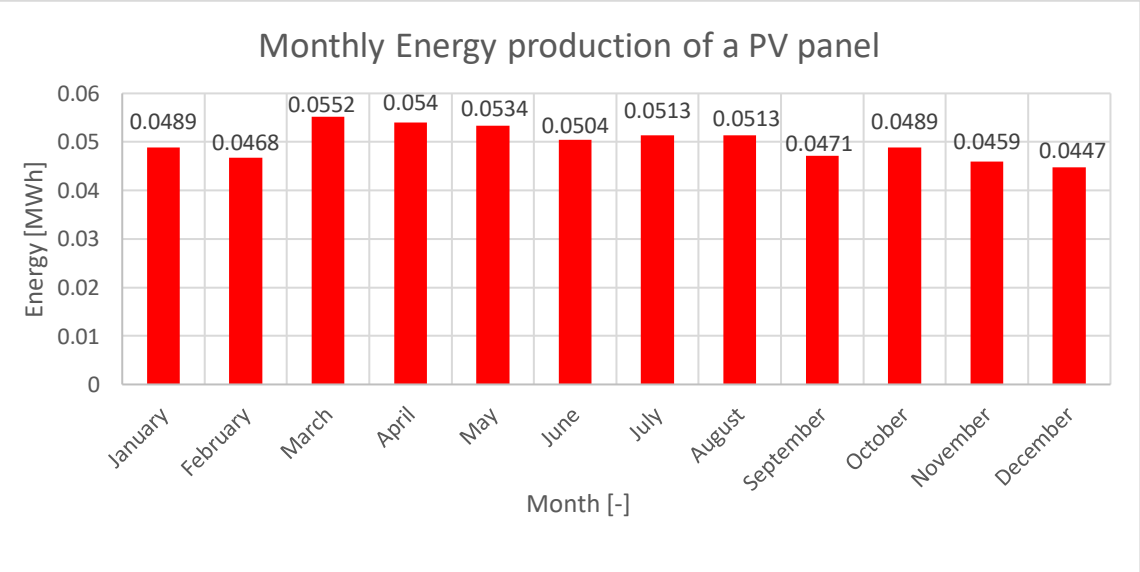


Figure 31: Monthly Energy Production of the PV panel

3.2.3 Storage System

The storage system considered in this study is based on a lithium ion (Li-ion) battery system: it is characterized by a high storage efficiency of up to 95% and high cycle stability of 1000-5000 cycles. The storage is an important part of a hybrid renewable plant because permits to meet the load demand in case of a low or insufficient energy production of the “generation side” (in this case represented by the PV-WIND system). In this way, it is possible to guarantee an interrupted energy supply to the load and helps, together with the choice of a hybrid system, to solve the intermittence’s issue of the renewable plant: so, the load demand, in this study represented by the electrolysers-system, can be met for every hour of the considered time period.

The sizing process used in this study is based on calculating the energy produced by the renewable system and the energy required by the electrolysers considering some constrains related to the Li-ion battery system.

In particular, the PV and WIND mathematical models allow evaluating the power and the amount of energy generated by renewable system at every time step ($E(t)_{gen}$): the total energy generated can be obtained by the sum of the energy produced by the PV panels ($E(t)_{PV}$) and WTs ($E(t)_{WT}$).

$$E(t)_{gen} = E(t)_{PV} + E(t)_{WT} \quad (12)$$

At the same time step, in this analysis considered equal to 1 hour, the electrolysers-system, constant for each time step, it has been computed and analysed in the following section of the work.

The mathematical model of the battery bank system is described by the State of Charge (SOC) of the batteries which counts, at any time (t), the amount of energy accumulated by the batteries. The values of the SOC can be only varied in the following range:

$$SOC_{min} \leq SOC(t) \leq SOC_{max} \quad (13)$$

where the SOC_{max} is the maximum battery capacity while the SOC_{min} is the minimum battery capacity, in this case considered equals to $0.2 \cdot SOC_{max}$, being a good practice not to fully discharge the battery in order to prevent its deterioration very quickly.

| | |
|--|-----|
| SOC_{max} [%] | 100 |
| SOC_{min} [%] | 20 |

Table 15: SOC_{max} and SOC_{min} of the considered Storage system

The SOC at each time step, $SOC(t)$, can be evaluated in the following way:

$$SOC(t) = \frac{E(t)_{bat}}{E_{bat,max}} \cdot 100 \quad (14)$$

Where

$E(t)_{bat}$: is the energy contained in the battery at time t, [MWh];

$E_{bat,max}$: is the maximum energy containable in the battery equals to its maximum capacity, [MWh];

Furthermore, considering a minimum SOC of 20%, the battery's parameter related to the Depth of Discharge (DoD) is equal to 80%.

In the event that the SOC, in a specific hour, is greater than the SOC_{max} there is a rate of energy that cannot be accumulated in the storage system and so, it is necessarily lost, while in case of the SOC is lower than the SOC_{min} , the energy accumulated in the storage system must be limited at least to its minimum value.

At each hour, the output energy, $E(t)_{gen}$, is calculated and compared to $E(t)_{load}$ and if $E(t)_{gen}$ is greater than $E(t)_{load}$ the battery is charging, otherwise it is discharging. This can be summarized with the following mathematical equations:

$$E(t)_{bat} = E(t-1)_{bat} \cdot (1 - \sigma) + [E(t)_{gen} - E(t)_{load}] \cdot \eta_{bat}^c \quad (15)$$

$$E(t)_{bat} = E(t-1)_{bat} \cdot (1 - \sigma) + [E(t)_{load} - E(t)_{gen}] / \eta_{bat}^D \quad (16)$$

The equation (15) represents the charging process, while the equation (16) represents the discharging process of the battery system. The η_{bat}^c is the charging efficiency of the battery, the η_{bat}^D is the discharging efficiency of the battery, while the σ is a parameter indicating the hourly self-discharge rate. Generally, the manufacturer documentation gives a self-discharge of 0.14% per day [25].

All the parameters mentioned for the battery system have been showed in the following table, while in **Table 17**, the datasheet of a Li-ion battery selected for this work has been reported [26].

| | |
|--------------------------------------|------|
| DoD [%] | 80 |
| η_{bat}^C [%] | 95 |
| η_{bat}^D [%] | 100 |
| σ [%/day] | 0.14 |

Table 16: Parameters used for the mathematical model

| TECHNICAL DATA | 1 Li-ion Battery (HOPPECKE) |
|------------------------------|-----------------------------|
| Technology | Li-ion module |
| Nominal Voltage [V] | 24 |
| Nominal Capacity [Ah] | 50 |
| Nominal Capacity [Wh] | 1200 |
| SOC_{min} [%] | 20 |
| SOC_{max} [%] | 100 |
| DoD [%] | 80 |
| Number of cycles [-] | 2500 |
| Efficiency [%] | 95 |

Table 17: Datasheet of the selected Li-ion battery [26]

The mathematical model assumed for the storage system and processed with a computer code using *Matlab Software* can be summarized with the following flow chart.

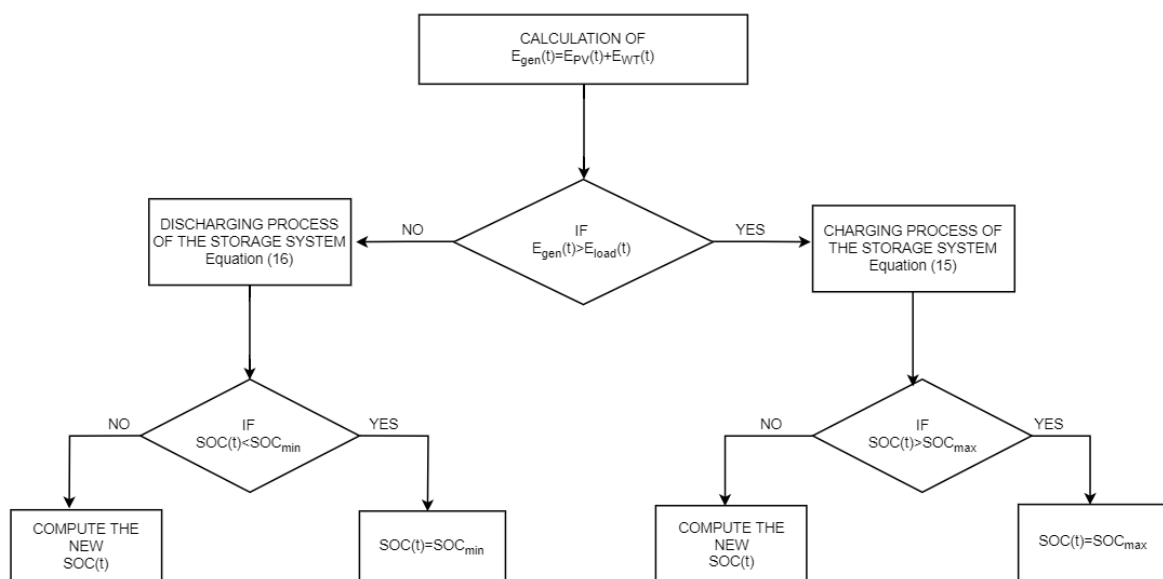


Figure 32: Flow Chart of the Storage system's model

For the mathematical model of the storage system it has been considered, as starting point³³, a SOC equal to 100%. Therefore, the storage system starts to work fully charged. The PV-WIND-STORAGE system has been sized to meet every hour the load demand.

In order to size the storage system, it is also necessary to find the total capacity of the storage system and so, also the total number of the batteries forming the system: the mathematical expression adopted for this goal will be exposed in the optimization analysis.

3.2.4 Electrolysers' System

The electrolysis is a process which permits to split the water's molecule into its constituents: the hydrogen (H₂) and oxygen (O₂) using electricity. The hydrogen production using electrolysis process can be totally renewable, as in this study, thanks to the electricity generation of a hybrid renewable plant constituted by a PV-WIND-STORAGE system. The available Water Electrolyser (WE) technologies can be classified according to its electrolyte into:

- Alkaline Electrolysers (AWE), in which the electrolyte is a liquid;
- PEM (Proton Exchange Membrane) Electrolysers (PEMWE), in which the electrolyte is a solid;
- Solid Oxide Electrolysers (SOWE).

Among these technologies, only AWE and PEMWE have enough maturity to find commercial units and between these two technologies, alkaline electrolysis is the oldest and more mature one. However, the model proposed here is based on a PEM electrolyser due to the different studies evolving the PEM technology in case of photovoltaic and wind sources for the electricity generation [15,29,30,31] and due to its big advantages: it can operate more flexibly and reactively than current AWE technology and it does not use hazardous chemicals and therefore the plant management is much easier. Moreover, the PEM electrolysers produce hydrogen at higher pressure (typically around 30 bar) than Alkaline electrolysers, which produce hydrogen at pressures up to 15 bar. This makes the PEM technology suitable for widespread use, in conjunction with renewable energy sources [32], but its disadvantage is the high cost if compared to that of alkaline electrolyser³⁴.

In this study, in order to compute the energy required by the electrolysers' system (load demand) at each hour, the following assumptions must be taken into account:

- 1) The hourly load demand is considered constant for the whole analysed period (1 year) and so this presumes a constant hydrogen production throughout the year;

³³ The starting point for the SOC of a storage system influences the "activity" evaluation and the design of the storage.

³⁴ The high cost of a PEM electrolyser is due to the nature of its catalyst: Platinum.

- 2) The sizing of the electrolysers' system is performed only considering the exploitation of the 70% of the total transport capacity of the *Transmed pipeline*: this choice is based on the statistical data considered in the previous section (section 2.1.2) related to the natural gas (NG) import from Algeria to Italy through Transmed during the analysed years (2010-2017). The sizing of the hybrid renewable plant could also be carried out considering the transport capacity of the other two pipelines starting from Hassi R'Mel (Medgaz and MEG) but, in this work, was decided to consider only the Transmed transport capacity in order to limit the size of the whole hybrid plant;
- 3) The hydrogen content within the gas blend (H₂ - NG) is limited to 2 vol%: up to 20% mixture of H₂ by volume in natural gas bulk doesn't cause any problems and only negligible adjustments to the infrastructures are necessary (this topic has been explained in the previously section of the work);
- 4) The output pressure of the produced hydrogen is assumed equals to 50 bar and therefore this allows its direct injection into the pipelines' network without an additional compression process;
- 5) In order to supply the required amount of the water to the electrolysers' system, it has been assumed the presence or the construction of a water desalination plant not far from the designed system.

After these considerations, it's possible to proceed with the mathematical model used for the sizing of the electrolysers' system (load demand).

First, the required amount of hydrogen should be calculated. This can be done accordingly to the assumption/considerations previously exposed (2nd and 3rd assumptions).

The obtained hydrogen value has been reported in the following table (in yellow) together with the densities at standard conditions³⁵ (*) of the hydrogen and natural gas, the total and the considered transport capacity of the *Transmed*.

| | |
|---|-------------|
| Total transport capacity of the TRANSMED pipeline [bcm/y] | 33 |
| Exploitation of the 70% of the TRANSMED transport capacity [bcm/y] | 23.1 |
| Density of natural gas*, ρ_{NG} [kg/m³] | 0.71682 |
| Density of hydrogen*, ρ_{H_2} [kg/m³] | 0.08989 |
| Yearly required amount of hydrogen [m³/y] | 462 000 000 |
| Yearly required amount of hydrogen [ton/y] | 41529.18 |

Table 18: The required amount of hydrogen for its transportation in pipeline

³⁵ The standard conditions for a gas are: temperature of 25°C and pressure of 1 atm.

The electrical power of the electrolysers' system has been computed by imposing a constant hydrogen production equal to 1.317 kg/s (q_{H_2}), according to the value reported (in yellow) in **Table 18**, while the used mathematical expression is:

$$P_{el} = \frac{q_{H_2} \cdot HHV_{H_2}}{\eta_{el}} \quad (17)$$

Where

P_{el} : is the total electrical power required by the electrolysers' system, [MW];

q_{H_2} : is the required amount of hydrogen, [kg/s];

HHV_{H_2} : is the Higher Heating Value of hydrogen, equals to 141.8 MJ/kg, [MJ/kg];

η_{el} : is the PEM electrolyser's efficiency assumed equals to 89%, [%].

With the total electrical power (P_{el}) and the hourly required amount of hydrogen, it has also been possible to obtain the energy consumed by the electrolysers' system per kg of produced hydrogen and, therefore, the total energy required by the load demand in 1 year (E_{load}).

The result of equation (17) together with the value of energy required by the load demand have been showed in the following table.

| | |
|--|------|
| P_{el} [MW] | 210 |
| E_{load} [kWh/kg_{H2}] | 44.3 |
| E_{load} [GWh/y] | 1838 |

Table 19: Results obtained for the Load demand

Therefore, the hourly energy required by the load is 0.2098 GWh/h: constant for each hour of the year. The required amount of the water for the electrolysers' system has been calculated assuming an inlet consumed water of 0.394 m³/MWh (value referred to the scientific document [15]) and, therefore, the annual amount of the consumed water is approximately 724 158 m³/y.

4. Optimization analysis of the hybrid system

In this section an optimization analysis, in terms of “*Levelized Cost of Electricity*” (LCOE), of the whole hybrid renewable plant has been carried out with a computer code generated on *MATLAB Software*.

The optimization analysis has the purpose to find the best configuration of the PV-WIND-STORAGE system which results in the lowest LCOE according to an optimal mix of the energy sources. In order to achieve this goal, 11 possible configurations of the hybrid system have been considered: percentages of installed capacity and, therefore, annual energy production of the PV SYSTEM and WT SYSTEM were varied for each configuration. The percentage of annual energy produced by each sub-system can be established considering one of the two following deterministic approaches:

- a) **ON ANNUAL BASIS:** the annual energy required by the electrolysers’ system (annual load demand³⁶: 1843 GWh/y) is shared between the PV and WT systems imposing that part of the annual load demand is covered by one sub-system and the remaining part by the other;
- b) **ON MONTHLY BASIS:** in this case, the monthly load demand, on a basis of 31 days (156 GWh/month), is considered by ensuring that also during the month with lower energy production for the PV and WT systems, each of the two sub-systems must be able to produce the % of monthly required energy. This can be summarized with the following equation:

$$E_{PV\ SYSTEM}(1\ month) + E_{WT\ SYSTEM}(1\ month) \geq E_{LOAD}(1\ month) \quad (18)$$

With the first approach, the required installed power of the hybrid system is lower respect to the installed power obtained with the 2nd approach: this means that the annual load demand of the electrolysers’ system can be covered with a smaller number of WTs and PV panels, but a higher nominal capacity of the STORAGE SYSTEM is necessary due to the fact that the annual energy generated by the PV-WIND system is exactly the same of that required by the load. The second approach is characterized by a higher number of WTs and PV panels, but the nominal capacity required by the storage system is lower: the annual energy generated by the PV-WIND system is higher than the annual load demand.

In order to limit the required nominal capacity of the STORAGE SYSTEM due to its high impact on the total costs of the hybrid plant, the optimization analysis is performed considering the 2nd approach (“on monthly basis”).

³⁶ The analysed time period is the 2020 (“Future scenario”): a leap year.

In the following table are showed the values of the monthly energy production of the WT and PV panel³⁷, in the analysed site (Hassi R'Mel, Algeria), so that it's possible to detect the worst months in terms of productivity for the PV and WT SYSTEM.

| | 1 WT [MWh] | 1 PV PANEL [MWh] |
|------------------|-----------------------|-----------------------------|
| JANUARY | 486.043 | 0.0489 |
| FEBRUARY | 480.741 | 0.0468 |
| MARCH | 665.493 | 0.0552 |
| APRIL | 869.074 | 0.0540 |
| MAY | 806.103 | 0.0534 |
| JUNE | 558.530 | 0.0504 |
| JULY | 557.416 | 0.0513 |
| AUGUST | 493.508 | 0.0513 |
| SEPTEMBER | 503.247 | 0.0471 |
| OCTOBER | 402.306 | 0.0489 |
| NOVEMBER | 399.213 | 0.0459 |
| DECEMBER | 543.627 | 0.0447 |

Table 20: Monthly energy production

The worst months in terms of productivity for the WT SYSTEM and PV SYSTEM are November and December, respectively.

As previously exposed, according to the approach based on the monthly load demand (2nd approach), the share of the energy produced by each of the two renewable sub-system has been established and the 11 proposed configurations reported in the following table together with their installed powers and annual energy productions.

| CONFIGURATION | WT SYSTEM [%] | PV SYSTEM [%] | WT SYSTEM [MW] | PV SYSTEM [MW] | N° WTs [-] | N° PV PANELS [-] | WT+PV SYSTEM [GWh/y] |
|----------------------|------------------------------|------------------------------|-------------------------------|-------------------------------|---------------------------|---------------------------------|-------------------------------------|
| 1 | 100 | 0 | 1176 | 0 | 392 | 0 | 2652 |
| 2 | 90 | 10 | 1056 | 105 | 352 | 349220 | 2591 |
| 3 | 80 | 20 | 939 | 210 | 313 | 698439 | 2535 |
| 4 | 70 | 30 | 822 | 314 | 274 | 1047659 | 2479 |
| 5 | 60 | 40 | 705 | 419 | 235 | 1396878 | 2424 |
| 6 | 50 | 50 | 588 | 524 | 196 | 1746097 | 2368 |
| 7 | 40 | 60 | 471 | 629 | 157 | 2095317 | 2313 |
| 8 | 30 | 70 | 354 | 733 | 118 | 2444536 | 2258 |
| 9 | 20 | 80 | 237 | 838 | 79 | 2793755 | 2202 |
| 10 | 10 | 90 | 120 | 943 | 40 | 3142975 | 2147 |
| 11 | 0 | 100 | 0 | 1048 | 0 | 3492194 | 2085 |

Table 21: Configurations analysed of the hybrid plant

³⁷ The monthly energy production is referred to the same WT and PV panel previously analysed: 1 WT of 3 MW and 1 PV panel of 300 W.

Among the 11 different configurations, the most productive is the 1st configuration: the configuration only formed by the WT SYSTEM. It is possible to see (**Table 21**) how the values related to the annual energy production tend to decrease with the decrease of the % of the used wind source reaching the minimum productivity value with the 11th configuration: only formed by the PV SYSTEM.

4.1 Calculation method for the nominal capacity of the Storage system

The storage system considered in this study is composed by a series of Li-ion batteries' bank with the technical specifications previously exposed. In order to meet the load demand, for each hour of the year, the pv-wind-storage system must guarantee the following condition:

$$E_{PV\ SYSTEM}(t) + E_{WT\ SYSTEM}(t) + E_{STORAGE\ SYSTEM}(t) \geq E_{LOAD}(t) \quad (19)$$

With the aim of finding the nominal capacity of the storage system that respect this condition, for each of the 11 examined configurations, the following calculation method has been developed.

The nominal capacity of the storage system has been computed taking into account the “worst condition” that may occur during the year for each configuration: this means the maximum registered daily mismatch between the production and the load demand when the load demand is higher than the energy production of the PV and WT SYSTEM [33]:

$$E_{LOAD}(1\ day) > E_{PV\ SYSTEM}(1\ day) + E_{WT\ SYSTEM}(1\ day) \quad (20)$$

$$mismatch = E_{LOAD}(1\ day) - [E_{PV\ SYSTEM}(1\ day) + E_{WT\ SYSTEM}(1\ day)] \quad (21)$$

The storage system's nominal capacity is computed considering both the characteristics of a single Li-ion battery formed the storage system and also the condition exposed above:

$$C_{STORAGE\ SYSTEM}^{nom} = \frac{\varphi \cdot mismatch}{DoD \cdot \eta_{batt}} \quad (22)$$

Where

DoD : Depth of Discharge of a single Li-ion battery, [-];

η_{batt} : efficiency of a Li-ion battery, [-];

$mismatch$: maximum difference between the load demand of the electrolysers' system and the energy production of the PV-WIND system, as expressed in the equation (21), [GWh/day];

φ : variable integer parameter, dependent on the analysed configuration, which defines the number of days (during the year) that must be considered to meet the load demand for each hour of the year, [days].

Analysing the data related to the hourly energy production of the hybrid system, thanks to the *Matlab Software*, has been possible to find the maximum daily mismatch for each of the 11 configurations, as show in this table.

| CONFIGURATION | WT SYSTEM [%] | PV SYSTEM [%] | N° WTs [-] | N° PV PANELS [-] | DAILY LOAD DEMAND [GWh/day] | MAXIMUM DAILY MISMATCH [GWh/day] |
|---------------|---------------|---------------|------------|------------------|-----------------------------|----------------------------------|
| 1 | 100 | 0 | 392 | 0 | 5.0355 | 5.0355 |
| 2 | 90 | 10 | 352 | 349220 | 5.0355 | 4.5514 |
| 3 | 80 | 20 | 313 | 698439 | 5.0355 | 4.4529 |
| 4 | 70 | 30 | 274 | 1047659 | 5.0355 | 4.3575 |
| 5 | 60 | 40 | 235 | 1396878 | 5.0355 | 4.2621 |
| 6 | 50 | 50 | 196 | 1746097 | 5.0355 | 4.1667 |
| 7 | 40 | 60 | 157 | 2095317 | 5.0355 | 4.0712 |
| 8 | 30 | 70 | 118 | 2444536 | 5.0355 | 3.9758 |
| 9 | 20 | 80 | 79 | 2793755 | 5.0355 | 3.8804 |
| 10 | 10 | 90 | 40 | 3142975 | 5.0355 | 3.7850 |
| 11 | 0 | 100 | 0 | 3492194 | 5.0355 | 3.6905 |

Table 22: Daily mismatch computed for each of the 11 configurations

The maximum daily mismatch is registered for the configuration only composed by the WT system with a value coinciding with that of the daily load demand: this means that in case of the 1st configuration (only WT system), there is at least one day, during the analysed year, in which there is no energy production because the wind speed will be lower respect to the *cut-in* speed required by the WTs. An opposite situation occurs in case of a system only formed by the PV (11th configuration). In case of 100% photovoltaic, in fact, the daily mismatch presents its minimum value, a value lower than the daily energy required by the electrolysers' system. This means that, with the configuration only composed by the PV system, there will be no day (during the year) characterized by a zero-energy production in the selected site, but the deficit will be given only for the night hours or for the hours with a low level of sunlight. In general, the daily mismatch decreases with the increment of the % of photovoltaic used in the energy

mix: this is due to the greater stability of the solar source in terms of energy production respect to that of the wind.

From this preliminary analysis, it's possible to imagine that the 1st configuration will be also the configuration with the higher value of the nominal capacity required by the storage system due to its higher daily mismatch.

After calculating the maximum daily mismatch, it has been necessary to estimate the value of ϕ (integer parameter) in order to obtain the nominal capacity of the storage system which permits to meet (for each configuration) the load demand every hour of the year. Thanks to the *Matlab Software* has been possible to generate a computer code which permits to obtain the value of ϕ for each of the eleven configurations and then the nominal capacities of the considered hybrid systems have been computed with the equation (22).

The ϕ parameter was varied between only integer values representing the days required by the hybrid system for meeting the load demand every hour.

A flow chart of the generated computer code is showed in the following page, while the results for the storage system's nominal capacities have been reported in **Table 23**.

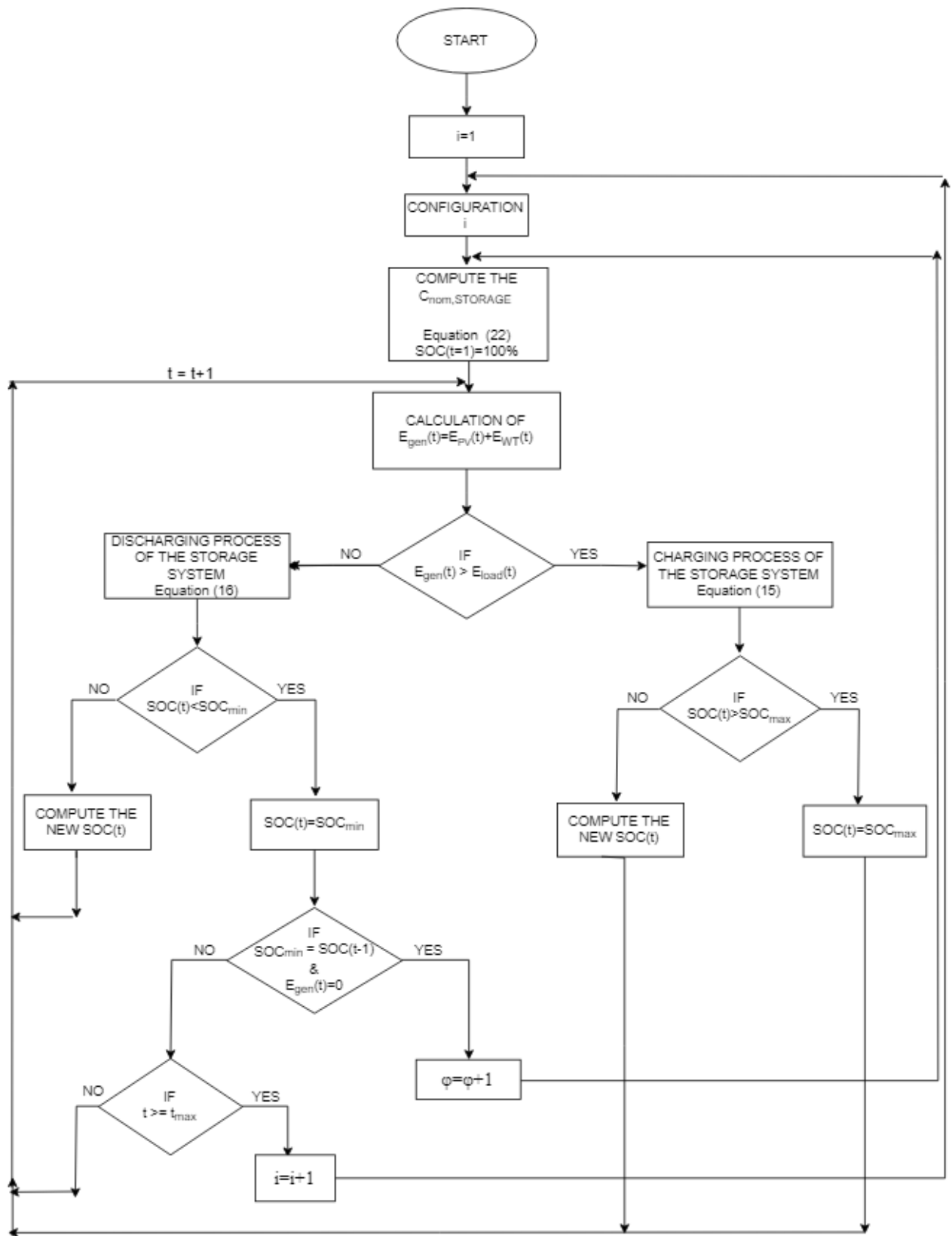


Figure 33: Flow Chart of the generated computer code with Matlab Software

| CONFIGURATION | WT SYSTEM [%] | PV SYSTEM [%] | DAILY LOAD DEMAND [GWh/day] | MAXIMUM DAILY MISMATCH [GWh/day] | ϕ PARAMETER [days] | NOMINAL CAPACITY OF THE STORAGE SYSTEM [GWh] |
|---------------|---------------|---------------|-----------------------------|----------------------------------|-------------------------|--|
| 1 | 100 | 0 | 5.0355 | 5.0355 | 9 | 59.631 |
| 2 | 90 | 10 | 5.0355 | 4.5514 | 9 | 53.898 |
| 3 | 80 | 20 | 5.0355 | 4.4529 | 8 | 46.873 |
| 4 | 70 | 30 | 5.0355 | 4.3575 | 7 | 40.135 |
| 5 | 60 | 40 | 5.0355 | 4.2621 | 6 | 33.648 |
| 6 | 50 | 50 | 5.0355 | 4.1667 | 6 | 32.895 |
| 7 | 40 | 60 | 5.0355 | 4.0712 | 5 | 26.784 |
| 8 | 30 | 70 | 5.0355 | 3.9758 | 4 | 20.925 |
| 9 | 20 | 80 | 5.0355 | 3.8804 | 4 | 20.423 |
| 10 | 10 | 90 | 5.0355 | 3.7850 | 3 | 14.941 |
| 11 | 0 | 100 | 5.0355 | 3.6905 | 5 | 24.280 |

Table 23: Nominal Capacity of the STORAGE SYSTEM for each configuration

The configuration with the lowest value of the ϕ parameter and, therefore, also with the lowest required nominal capacity of the storage system is the **configuration 10** formed by the 90% of the photovoltaic and 10% of the wind source. This means that a hybrid configuration of the two renewable sub-systems, for specific % of the involved photovoltaic and wind source, produces advantages in terms of size of the required storage system. A specific combination of the PV and WT system needs a lower size of the storage system respect to that obtained with the only WT system (1st configuration) or only PV system (11th configuration).

Thanks to the value of the nominal capacity of the storage system, it is also be possible to find the number of the required Li-ion batteries composing the system:

$$N_{bat} = \frac{C_{STORAGE\ SYSTEM}^{nom}}{C_{1\ bat}^{nom}} \quad (23)$$

Where

N_{bat} : number of Li-ion batteries, [-];

$C_{STORAGE\ SYSTEM}^{nom}$: obtained nominal capacity of the storage system, [GWh];

$C_{1\ bat}^{nom}$: nominal capacity of a single Li-ion battery, [GWh];

4.2 “Levelized Cost of Electricity” (LCOE) of the different configurations

The aim of the optimization analysis is to evaluate and find the configuration, among those analysed, that minimizes the “*Levelized Cost of Electricity*” (LCOE).

The LCOE of a system is an essential parameter representing the average revenue per unit of electricity generated, $\frac{\text{€}}{\text{kWh}}$ or $\frac{\text{€}}{\text{MWh}}$, that would be required to recover the lifetime costs of the system. The LCOE is a useful tool that allows the comparison of different technologies (e.g. wind, solar, natural gas, etc.) of unequal life spans, project size, different capital cost, risk, return and capacities. In order to estimate the LCOE of a specific technology, these key inputs are necessary:

- Capital costs;
- Fuel costs;
- Fixed and variable Operations and Maintenance (O&M) costs;
- Discount rate;
- Electricity generation;
- Economic life of the system.

The importance of each of these factors varies across the technologies. For technologies with no fuel costs and relatively small variable O&M costs, such as solar and wind electric generating technologies, LCOE changes nearly in proportion to the estimated capital cost of the technology. In case of technologies with significant fuel costs, the fuel costs and capital costs estimates significantly affect the LCOE.

The LCOE of renewable energy technologies varies by technology, Country and project, based on the renewable energy sources, capital and operating costs, and the efficiency/performance of the technology.

Data from the *IRENA Renewable Cost Database* [35] show that the global weighted-average LCOE of utility-scale solar PV, onshore and offshore wind has fallen between 2010 and 2018: the utility-scale solar PV projects commissioned in 2018 had a global weighted-average LCOE of $0.076 \frac{\text{€}}{\text{kWh}}$ which was around 13% lower than that of 2017 and 77% lower respect to the value of the 2010. In 2018, the global weighted-average LCOE of the onshore wind projects was $0.050 \frac{\text{€}}{\text{kWh}}$ (13% lower than that of 2017).

In order to have an idea of the LCOE value (expressed in $\frac{\text{USD}}{\text{kWh}}$) of the different renewable and fossil-fuel technologies according to the capacity (MW), the following figure of the “*International Renewable Energy Agency*” (IRENA) has been reported.

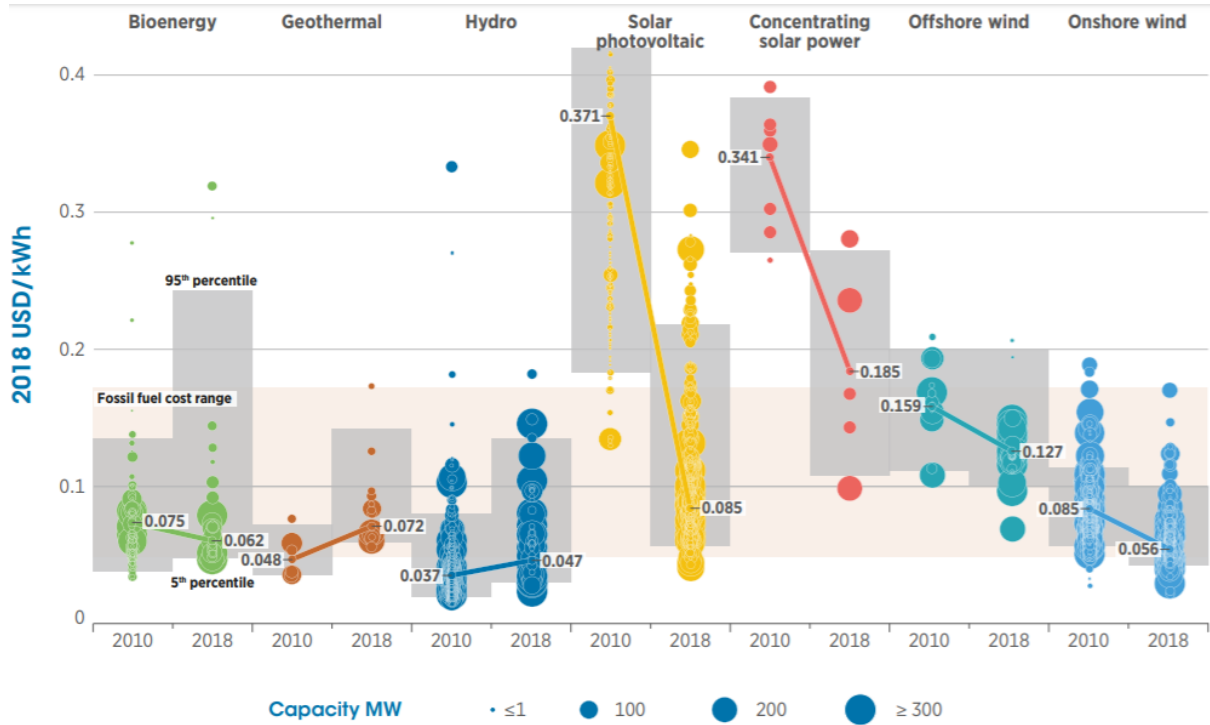


Figure 34: Global LCOE of utility-scale renewable power generation technologies, 2010-2018 [35]

In 2018, the global weighted-average LCOE for onshore wind, hydropower, bioenergy and geothermal projects commissioned were all at the lower-end of the fossil-fuel cost range, so that those technologies competed head-to-head with fossil fuels. With continued cost reductions, solar PV power has also started to compete directly with fossil fuels. Offshore wind and concentrating solar power (CSP) are less widely deployed, and their global weighted-average electricity costs are in the top half of the fossil fuel cost range [35].

In this study, in order to evaluate the LCOE of the different configurations, the following calculation for the *Levelized Cost of Electricity* has been adopted [42]:

$$LCOE = \frac{C_i + \sum_{t=1}^n O\&M_t \cdot (1+r)^{-t}}{\sum_{t=1}^n E_t \cdot (1+r)^{-t}} \quad (24)$$

$$C_i = C_{PV\ SYSTEM} \cdot P_{PV} + C_{WT\ SYSTEM} \cdot P_{WT} + C_{STORAGE\ SYSTEM} \cdot C_{nom,STORAGE} \quad (25)$$

$$O\&M_t = O\&M_{t,PV\ SYSTEM} \cdot P_{PV} + O\&M_{t,WT\ SYSTEM} \cdot P_{WT} + O\&M_{t,STORAGE\ SYSTEM} \cdot C_{nom,STORAGE} \quad (26)$$

$$E_t = E_{t,PV\ SYSTEM} + E_{t,WT\ SYSTEM} \quad (27)$$

Where

C_i : Capital Cost of the components of the hybrid plant, [€];

P : installed power of the component, [kW];

C_{nom} : Nominal Capacity of the storage system, [kWh];

$O\&M_t$: Operation and Maintenance costs including also the replacement costs for the storage system's batteries at time t, [€];

E_t : energy produced by the hybrid plant at time t, [kWh];

r : discount rate considered equal to 5%³⁸, [-];

n : lifetime of the whole hybrid system considered equal to 20 years, [y].

The total installed costs of each component formed the hybrid system have been extrapolated from the database of IRENA: these data show an important reduction of the total installed costs, especially for the PV and onshore WIND technologies, during the time period 2010-2018, but the total installed costs still represent the largest expenditure for the renewable technologies.

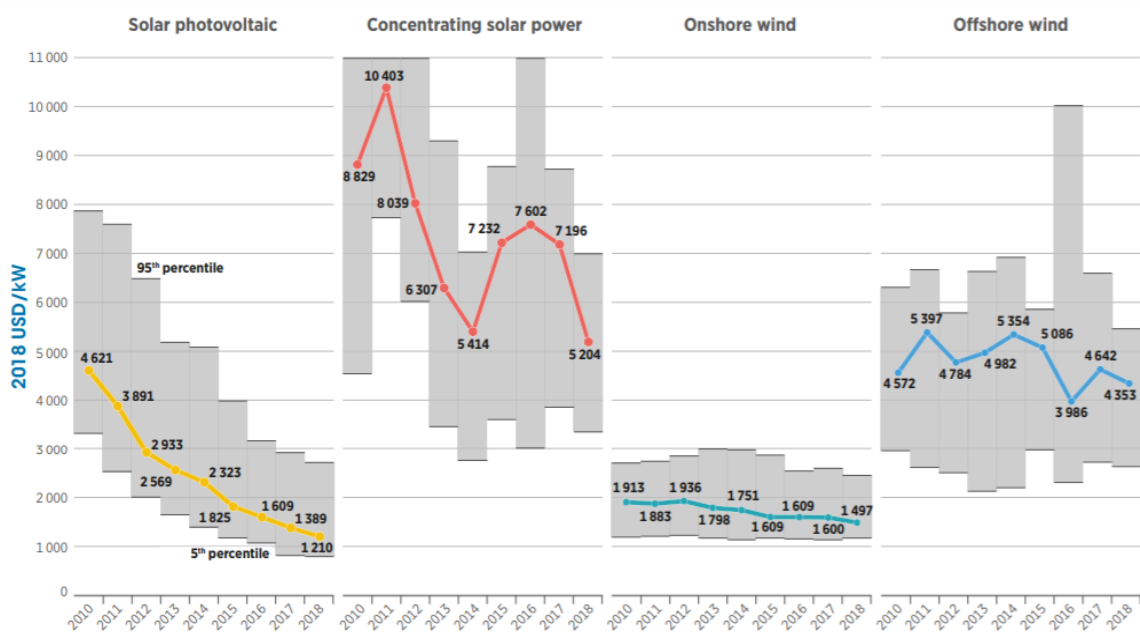


Figure 35: Global weighted average total installed costs and project percentile ranges for same renewable technologies [35]

³⁸ It is calculated basing on the financial structure of the investment and therefore it depends on: cost of equity (k_e) and cost of debt (k_d). The adopted mathematical relation has been taken from [43].

For the calculation of the LCOE, the values of the total installed costs, in case of PV and WT systems, are that referred to the year 2018, while the operation and maintenance costs (O&M) are expressed as percentage of the total installed costs for each renewable technology [15].

The costs of the Li-ion batteries forming the storage system are also extrapolated from the reports of IRENA [36] and, also in this case, an important cost reduction is evident (**Fig.36**). A table containing all the considered costs is reported (**Table 24**).

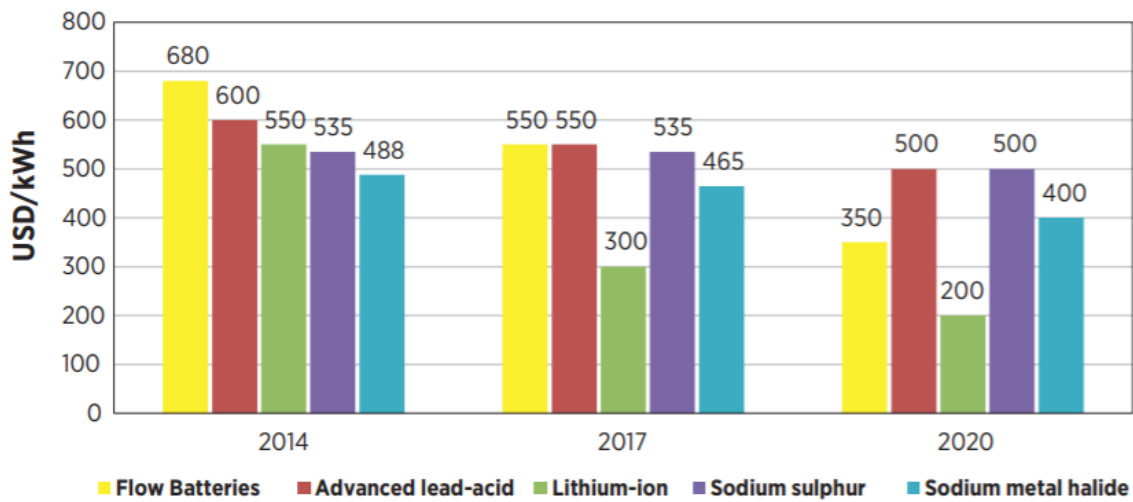


Figure 36: Battery price by type for utility-scale applications [36]

| | PV SYSTEM | WT SYSTEM | STORAGE SYSTEM |
|--------------------------------------|---------------------------|---------------------------|-------------------------|
| Capital costs, C [€/kW] | 1088 | 1346 | - |
| Capital costs, C [€/kWh] | - | - | 280 |
| Operation and Maintenance costs, O&M | 0.5% of the Capital costs | 1.5% of the Capital costs | 1% of the Capital costs |
| Operation and Maintenance costs, O&M | 5.44 €/kW | 20.19 €/kW | 2.8 €/kWh |
| Years of operations [years] | 20 | 20 | 10 |

Table 24: Considered costs for the calculation of LCOE of the PV-WIND-STORAGE SYSTEM

In the calculation of LCOE, the following simplifying assumptions are considered:

1. The annual production of the electrical energy (E_t) by the PV-WIND system is considered constant for the whole reference time period (20 years). This assumption presumes that each of the two sub-systems of the hybrid plant (PV and WT system) works for a determinate and constant number of the equivalent hours (h_{eq}) every year, for the whole considered time period. The equivalent hours (h_{eq}) represent the operational hours of the PV and WT system at their nominal power;
2. The discount rate, r , is assumed constant and equal to 5% for the whole analysed time period.

The obtained values of LCOE (eq. 24) for each configuration are showed in the following table.

| CONFIGURATION | WT SYSTEM [%] | PV SYSTEM [%] | NOMINAL CAPACITY OF STORAGE SYSTEM [GWh] | LCOE [€/kWh] |
|---------------|---------------|---------------|--|--------------|
| 1 | 100 | 0 | 59.631 | 0.625 |
| 2 | 90 | 10 | 53.898 | 0.582 |
| 3 | 80 | 20 | 46.873 | 0.522 |
| 4 | 70 | 30 | 40.135 | 0.463 |
| 5 | 60 | 40 | 33.648 | 0.404 |
| 6 | 50 | 50 | 32.895 | 0.403 |
| 7 | 40 | 60 | 26.784 | 0.344 |
| 8 | 30 | 70 | 20.925 | 0.284 |
| 9 | 20 | 80 | 20.423 | 0.283 |
| 10 | 10 | 90 | 14.941 | 0.224 |
| 11 | 0 | 100 | 24.280 | 0.341 |

Table 25: LCOE of the 11 analysed configurations of the hybrid plant

The result of the optimization analysis shows a minimum value of the *Levelized Cost of Electricity* for the **configuration** number **10** (90% of photovoltaic and 10% of wind source): this configuration presents also the minimum value of the nominal capacity of the storage system, this means that the costs of the STORAGE SYSTEM play an important role in the total costs of the pv-wind-storage plant. In particular, for the optimal configuration, the total costs (Capital, Operational and Maintenance costs) are represented by a 79% of the STORAGE SYSTEM's costs, 18% of the PV SYSTEM's costs and only a small portion, 3%, for the WT SYSTEM's costs.

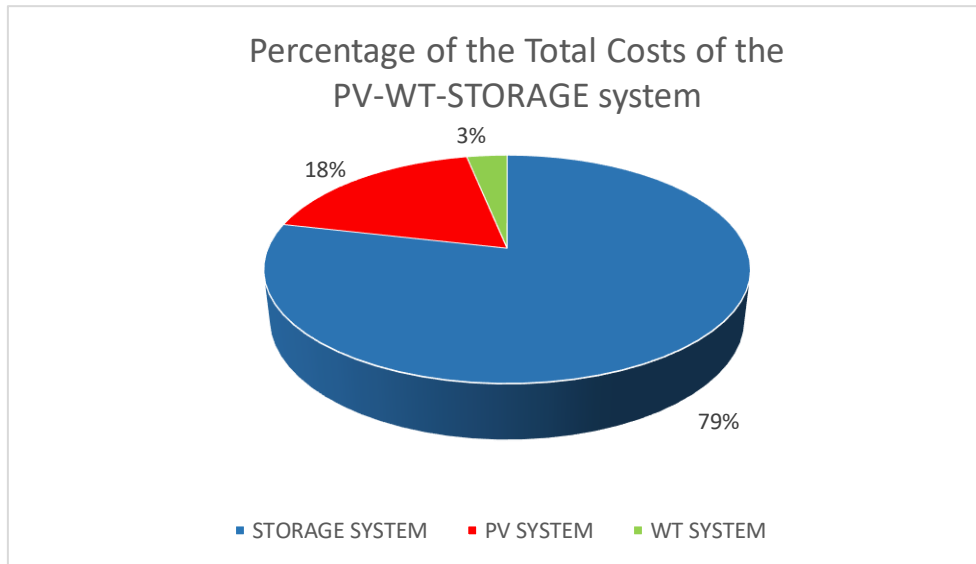


Figure 37: Percentage of the Total Costs of the Optimal PV-WIND-STORAGE SYSTEM configuration

The monthly energy production of the optimal pv-wind-storage system configuration (**configuration number 10**) together with the small monthly fluctuations of the load demand of the electrolysers' system (constant for each hour of the year) is showed below. In this study is not considered, but the energy surplus produced by the proposed hybrid system could be sold to the national power grid if the whole hybrid system was connected.

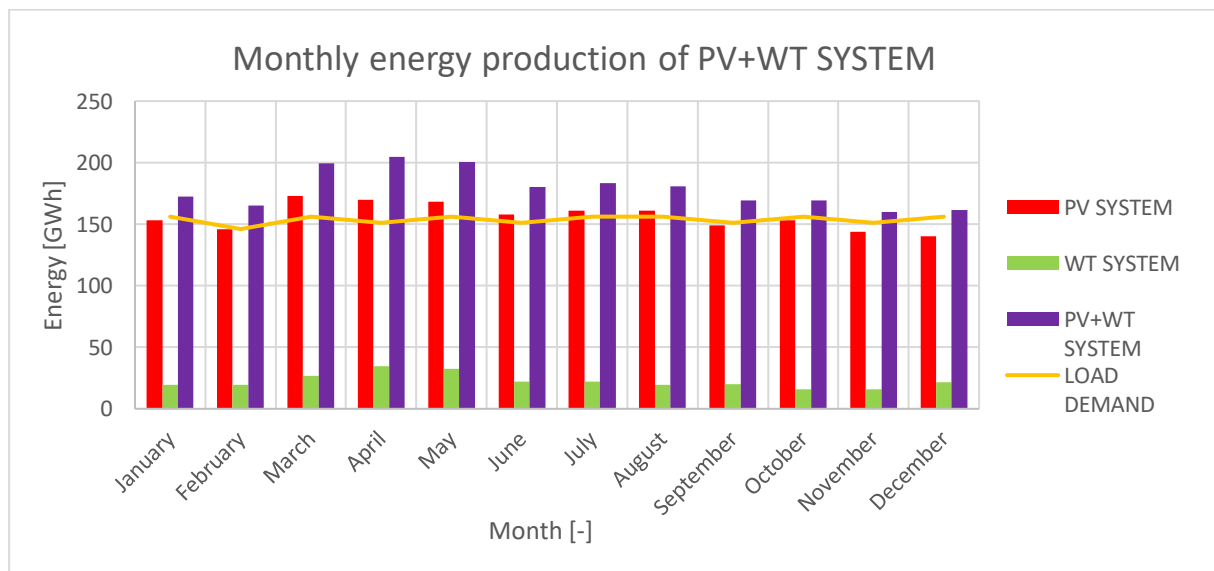


Figure 38: Monthly energy production of the optimal hybrid system

In order to evaluate also how the storage system works, an evolution of its State of Charge (SOC), during the year, is reported. The starting point for the SOC of the storage system is 100% ($SOC_{max}=100\%$ and $SOC_{min}=20\%$).

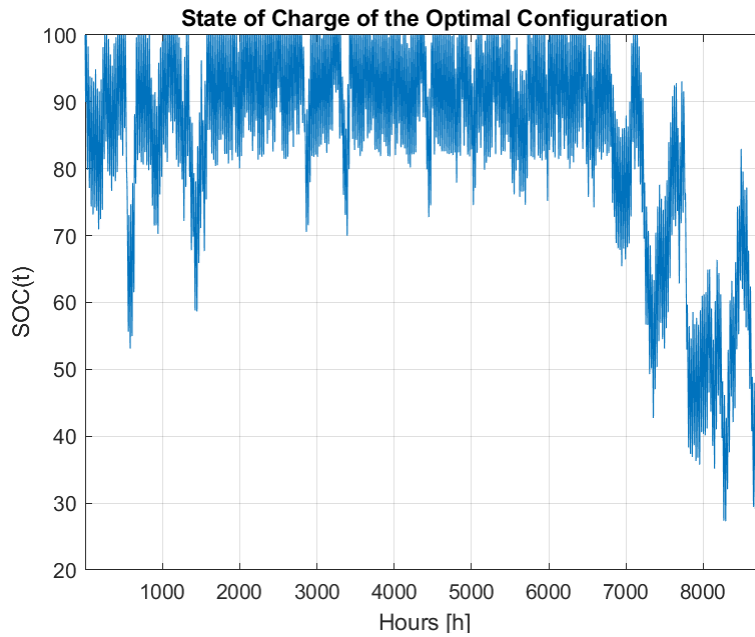


Figure 39: Evolution of the State of Charge (SOC) of the Optimal Configuration

The cost of the electrical energy produced only by the proposed WT and PV system, in the analysed site, is showed in the Table.

| | LCOE [€/kWh] |
|------------------|-------------------------|
| WT SYSTEM | 0.06 |
| PV SYSTEM | 0.05 |

Table 26: LCOE of the only WT and PV SYSTEM

In this study, the unit cost of the electrical energy produced by the WT system is slightly higher than the unit cost of the PV system. As previously discussed, the costs reduction of onshore wind and pv technologies drives the decline of the LCOE of these technologies. In particular, the auction data of the IRENA’s database suggests that the average price of the electricity, for utility-scale solar PV, could fall to 0.043 €/kWh in 2020: a reduction of 44% compared to the weighted-average LCOE of projects commissioned in 2018 [35], while in case of onshore wind technology its weighted-average LCOE, in 2020, remains approximately constant compared to that of 2018.



Figure 40: The LCOE for projects and global weighted average value [35]

4.3 “Levelized Cost of Hydrogen” (LCOH₂)

The “Levelized Cost of Hydrogen” (LCOH₂) produced by the proposed hybrid plant, in case of optimal PV-WIND-STORAGE system configuration (**configuration 10**), in this work has been computed using this mathematical relation:

$$LCOH_2 = \frac{C_i + \sum_{t=1}^n O\&M_t \cdot (1+r)^{-t}}{\sum_{t=1}^n E_t \cdot (1+r)^{-t}} \quad (28)$$

the terms showed in the equation (28) are the same of the equation (24), but also the costs related to the PEM electrolyzers’ system are included.

In this LCOH₂ calculation, the costs for the water consumption by the electrolyzers and for hydrogen transportation³⁹ are not considered.

³⁹ The costs for the hydrogen transportation, in this proposed study, are very low due to the localization of the analysed hybrid plant: the generation and injection sites are very close to each other. For this reason, the transportation costs can be neglected.

The capital costs and the Operational and Maintenance costs (O&M costs) of the electrolyzers' system are summarised in the following table (values referred to the scientific document [15] and compared to that of IRENA database [37]).

| | PEM ELECTROLYSERS-SYSTEM |
|---|---------------------------------|
| Capital costs, C [€/kW] | 1000 |
| Operation and Maintenance costs, O&M | 3% of the Capital costs |
| Operation and Maintenance costs, O&M | 30 |
| Years of operations [years] | 20 |
| Installed Power [MW] | 210 |

Table 27: Costs of PEM Electrolyzers' system [15]

The value obtained of LCOH₂ is the following.

| | |
|---------------------------------|--------------|
| LCOH₂ [€/kWh] | 0.235 |
|---------------------------------|--------------|

Table 28: Levelized Cost of Hydrogen (LCOH₂) produced by the proposed hybrid plant

The distribution of the total costs of the whole hybrid plant is showed below.

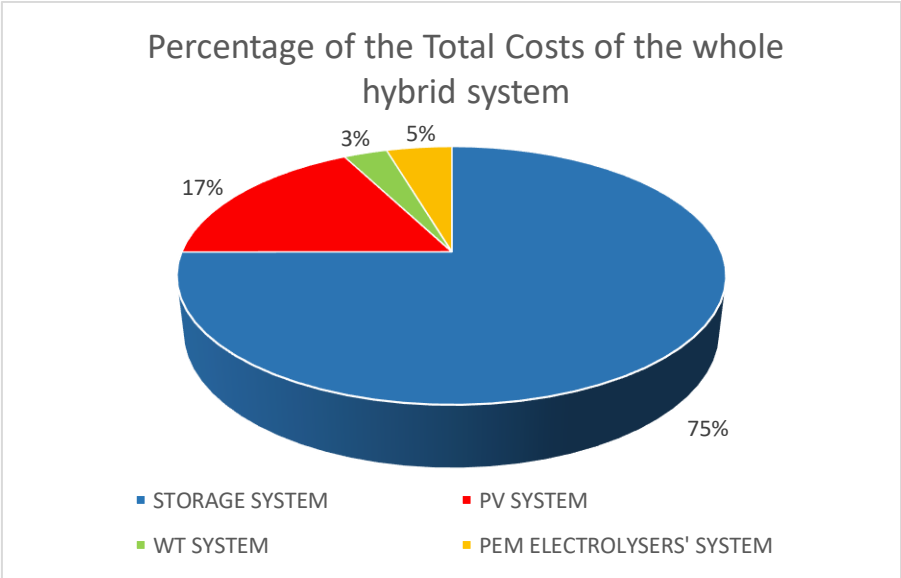


Figure 41: Percentage of the Total Costs of the whole hybrid plant

Considering a constant annual hydrogen production, equals to 41529.18 ton_{H2}/y, for the whole lifetime of the hybrid plant (20 years), the levelized cost of hydrogen per unit of produced kg is:

| | |
|---|-----|
| LCOH₂ [€/kg_{H2}] | 7.6 |
|---|-----|

Table 29: Levelized Cost of Hydrogen (LCOH₂) per unit of produced kg by the proposed hybrid plant

As previously discussed, the Levelized Cost of Hydrogen (LCOH₂) is mainly influenced by the costs related to the storage system of the hybrid plant due to the fact that a large nominal capacity of storage is required to allow a steady-state operation, for the whole time period, of electrolyzers. In order to evaluate the influence of storage system in the calculation of LCOH₂, the hydrogen production costs have been computed only considering:

- The costs related to the PV-WIND system and electrolyzers (without storage);
- The costs related to the PV-WIND system, electrolyzers and storage system with half of required nominal capacity.

The results are showed in the following figure.

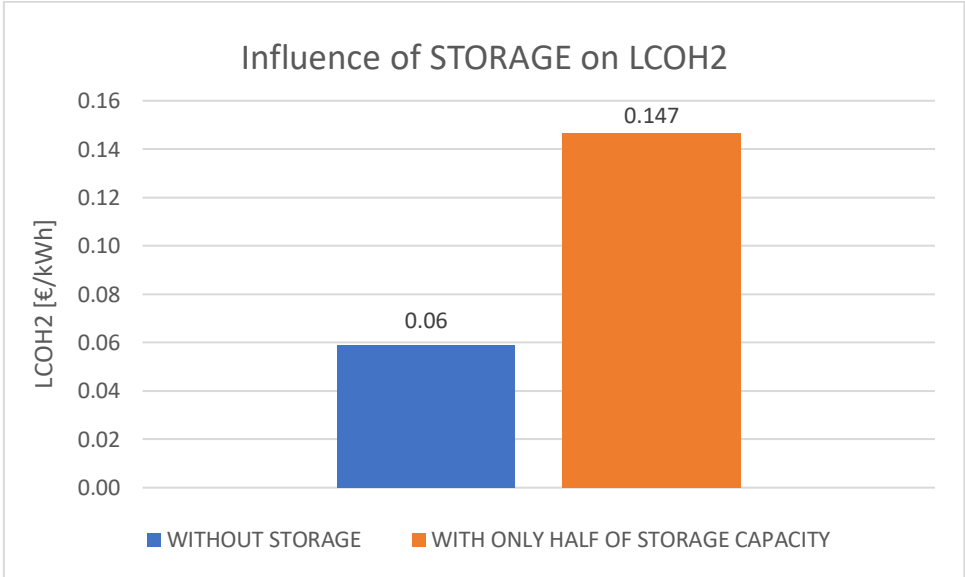


Figure 42: Influence of STORAGE costs on LCOH₂

Reducing the size of storage system (half of the required nominal capacity) means an important reduction for the LCOH₂: this value passes from 0.235 €/kWh to 0.147 €/kWh (-37.4%) with a cost, for each kg of produced hydrogen, of 4.7 €/kg_{H2}. For these reasons, design solutions of the hybrid plant that limit the size of storage system generate a significant cost reduction. For example, it is possible to see from the **Figure 39** that the proposed storage

system, for 7000 h of the analysed year, reaches a State of Charge (SOC) of approximately 54% as lowest value and, only in the last 1784 h of the year, lower values of SOC are involved until it reaches its minimum SOC (20%). This means that, for a great number of hours (approximately 7000 h/y), the storage system can work with only half of its nominal capacity and, therefore, for the last 1784 h/y, it is possible to think a different solution that involves a transient operation of electrolyzers. In this way, it is possible to obtain a lower size of storage system and an important reduction of hydrogen production costs.

In this study, it has been assumed a continuous steady-state system operation of PEM electrolyzers in order to supply a constant hydrogen production during the year, this means a utilization factor of 100%. Generally, to be competitive, the electrolyzers would have to have relatively high utilization factor: they would have to run for several thousand hours per year.

The following figure shows the LCOH₂ for PEM electrolyzers that are directly connected to renewable off-grid energy plant. Lower load factors (smaller bubble size in **Figure 43**) increase the LCOH₂.

Of course, the cost of hydrogen production is also affected by the adopted renewable technology (only PV, only WIND or a combination of them) and by the geographic site of the energy production. According to the IRENA reports, the target for the renewable hydrogen production is expected to be approximately of 3 USD/kg of H₂ in 2030.

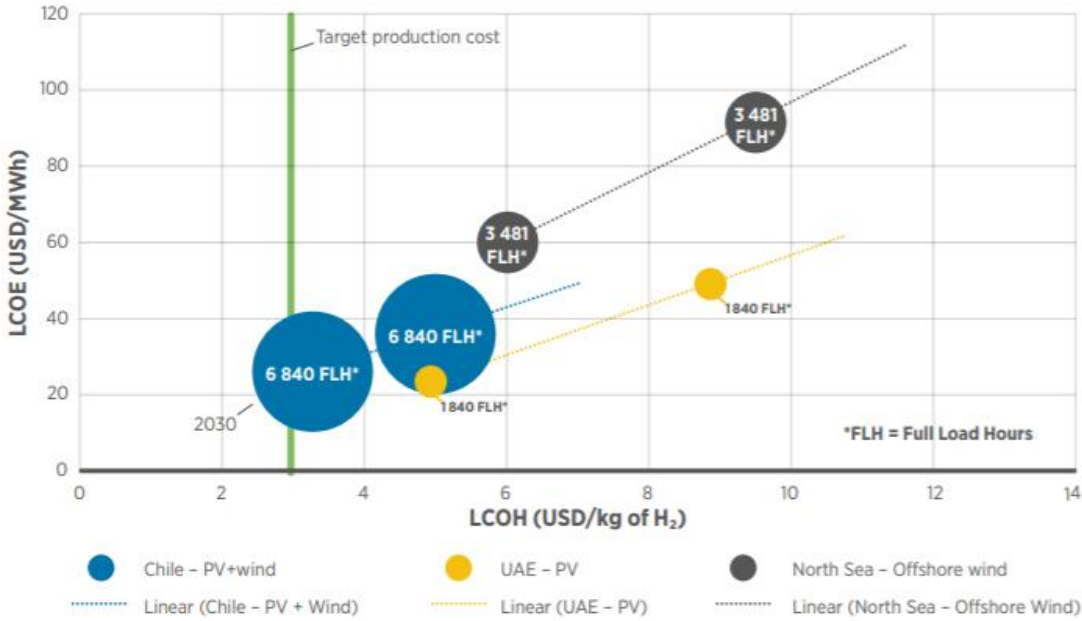


Figure 43: Cost of hydrogen as a function of cost of electricity and utilisation rate of PEM electrolyser [37] ⁴⁰

⁴⁰ UAE: United Arab Emirates; FLH: Full Load Hours.

In particular, countries such as Argentina (due to the high load factor of wind generation in Patagonia) and Australia and Chile (due to abundant sun) are developing roadmaps to convert their surplus variable renewable energy into compressed gaseous or liquid hydrogen (or another carrier similar to LCOH₂) for transport to regions with a net demand, such as Japan and the Republic of Korea [37].

Based on extensive wind and solar geospatial data, the figure below reveals vast areas (from light green to yellow and orange) where a combination of solar PV capacities and modern wind turbines combined would supply a load with load factors over 50%, and up to 6000 FLH or more in the few red areas.

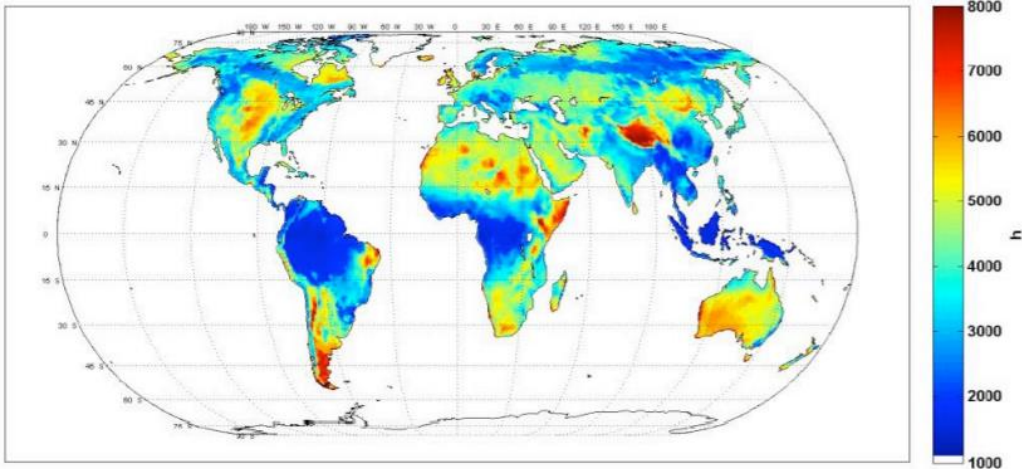


Figure 44: Hybrid solar and wind load factors [38]

5. Conclusions

The aim of this work is to investigate the option to produce renewable hydrogen from water electrolysis in North Africa. The whole hydrogen production process is based on renewable energy provided by PV panels and wind turbines (WTs) plus a storage system composed by batteries. The analysed option for the hydrogen transport is the existing natural gas infrastructure: the produced hydrogen is blended in the existing natural gas pipeline system and transported to Central Europe. At the moment, this transport option appears the most economically viable and most attractive for a transition towards an “Hydrogen Economy”. Assuming a 2% blend of hydrogen within the Transmed pipeline, connecting Algeria and Italy, changes or modifications of the pipelines’ network are not necessary. Due to the “hybrid nature” of the produced energy, an optimization criterion is developed in order to select the best configuration of the PV-WIND-STORAGE system in terms of unit cost of energy production. This optimization analysis is performed on a selected number of configurations of the hybrid plant (11 configurations) and by imposing same constraints for the choice of the components: WTs (3 MW), PV panels (300 W) and (Li-ion) batteries. An optimization analysis that considers a higher number of possible configurations of the hybrid plant and with a greater freedom’s degree on the size and type of the different components of the plant, would certainly produce a more accurate result.

From this study, the result of the optimization analysis provides a PV-WIND-STORAGE system configuration formed by a 90% photovoltaic and 10% wind with a LCOE equals to 0.224 €/kWh where the costs of the storage system represent the 79% of the total costs of the hybrid system. The cost of the energy produced by the WT and PV systems, in fact, are relatively low: 0.06 €/kWh and 0.05 €/kWh, respectively. For the renewable technologies, the total installed costs still represent the largest expenditure, but an important reduction of this has occurred during the years and a farther cost reduction is expected for the next future. The obtained result shows also the advantage of a solution based on a combination of the two renewable sources: solar and wind. This combination allows to limit the problem related to the intermittence of the two sources and, therefore, gives a more stable energy production. From the proposed hybrid system is obtained a “Levelized Cost of Hydrogen” (LCOH₂) of 7.6 €/kg of the produced hydrogen considering a continuous system operation of the (PEM) electrolyzers: this means an utilization factor of 100%. The Levelized Cost of Hydrogen depends on different factors, such as: load factors, technologies involved in the hydrogen production, geographic site of the energy generation, etc. In particular, the choice of the geographic site affects also the load factors of the adopted renewable technologies: there are vast areas, like some African regions, in which the combination of solar and wind sources produces load factors over 50-60% (higher than that occurred in this study). The target for the renewable hydrogen production, in 2030, is expected to be approximately of 3 USD/kg of H₂ and this means an important step for the development of the new “Hydrogen Economy”, but as long as hydrogen is blended to fossil natural gas and needs it as “carrier” in the pipelines, the import of fossil natural gas is still necessary, i.e. GHG (“Green House Gas”) emissions savings are limited.

6. References

- [1] I.E.A. (IEA), *“International Energetic Agency (IEA)”*, 2018
- [2] *“Organization of the Petroleum Exporting Countries (OPEC): Annual Statistical Bulletin 2018*
- [3] *Eurostat Database, European Statistics*
- [4] *“Ministero dello Sviluppo Economico – Analisi e Statistiche Energetiche”*, Governo Italiano
- [5] *“Ceic Data: Global Economic Data, Indicators, Charts and forecasts”*
- [6] *“Trans-Mediterranean Natural Gas Pipeline”*, Hydrocarbons Technology
- [7] *“Trans-Mediterranean Pipeline”*, Wikipedia
- [8] *“Study of management strategy of energy resources in Algeria”*, Zhour Abada, Malek Bouharkat, Department of Electrical Engineering, University of Batna 2, Algeria (2018)
- [9] *“Les énergies renouvelables en algérie: chiffres Clefs, service économique regional”*, Ambassade De France, Alger, Algérie, Sulmont, N., Meley, F., 2013^a
- [10] *“Energy and Mines Book 2007”*, www.mem-algeria.org
- [11] *“Renewable Energy Development Centre (CDER)”*, Algeria, www.cder.dz
- [12] *“Prospects of hydrogen production potential from renewable resources in Algeria”*, Soumia Rahmouni, Belkhir Negrou, Nouredine Settou, Javier Dominguez, Abderahman Gouareh
- [13] *Ministry of Energy, “Renewable energies and energy efficiency development program”*, January 2016
- [14] *“MedHySol: Future federator project of massive production of solar hydrogen”*, Bouziane Mahmaha, Farid Harouadia, H. Benmoussab, Samira Chadera, Maiouf Belhamela, Abdelhamid M’Raouia, Kamel Abdeladima, Adel Nasser Cheriguic, Claude Etievantd
- [15] *“Hydrogen from renewables: Supply from North Africa to Central Europe as blend in existing pipelines – Potentials and costs”*, Sebastian Timmerberg, Martin Kaltschmitt
- [16] *“Parabolic trough solar thermal power plant: Potential, and projects development in Algeria”*, Taqiy eddine Boukelia, Mohamed-Salah Mecibah
- [17] *WT’s Datasheet*,
<https://en.wind-turbine-models.com/turbines/603-vestas-v90-3.0#datasheet>
- [18] *Slides of “Power generation from renewable sources” course*, Prof. Filippo Spertino
- [19] *“Technical and economic assessment of wind farm power generation at Adrar in Southern Algeria”*, Said Diafa, Gilles Nottonb, Djamilia Diafa

- [20] *“Quaderni di applicazione tecnica N.13 – Impianti Eolici”*, ABB
- [21] *“A statistical investigation of wind characteristics and wind energy potential based on the Weibull and Rayleigh models in Rwanda”*, Bonfils Safari, Jimmy Gasore
- [22] *“Overview of PV-GIS data sources and calculation methods”*, European Commission, https://re.jrc.ec.europa.eu/pvg_static/methods.html
- [23] *“A power-rating model for crystalline silicon PV modules”*, Huld et al., 2011
- [24] *PV panel’s Datasheet*,
http://static.trinasolar.com/sites/default/files/LA_TSM_PD14_datasheet.pdf
- [25] *“Sizing methods and optimization techniques for PV-wind based hybrid renewable energy system: A review”*, Kamal Anoune, Mohsine Bouya, Abdelali Astito, Abdellatif Ben Abdellah
- [26] *Li-ion battery’s Datasheet*,
https://sun.hoppecke.com/content/download/brochures/mp/LiOnBatteriesysteme_en.pdf
- [27] *“A sizing approach for stand-alone hybrid photovoltaic-wind-battery systems: A Sicilian case study”*, Antonio Giallanza, Mario Porretto, Gabriella Li Puma, Giuseppe Marannano
- [28] *“Sizing of a stand-alone Photovoltaic/Wind Energy System with Hydrogen and Battery Storage based on Improved Ant Colony Algorithm”*, Weiqiang Dong, Yanjun Li, Ji Xiang
- [29] *“Performance of a PV–wind hybrid system for hydrogen production”*, Kamaruzzaman Sopian, Mohd Zamri Ibrahim, Wan Ramli Wan Daud, Mohd Yusof Othman, Baharuddin Yatim, Nowshad Amin
- [30] *“Techno-economic analysis of stand-alone photovoltaic/wind/battery/hydrogen system for very small-scale applications”*, Saša M. STOJKOVI and Vukman V. BAKI
- [31] *“Performance investigation of hydrogen production from a hybrid wind-PV system”*, E. Akyuz, Z. Oktay, I. Dincer
- [31] *“Concept of a high pressure PEM electrolyser prototype”*, F. Marangio, M. Pagani, M. Santarelli, M. Cali`
- [32] *Meteonorm 7.3 Manual*
- [33] *“Sizing stand-alone photovoltaic–wind hybrid system: Techno-economic analysis and optimization”*, Hocine Belmili, Mourad Haddadi, Seddik Bacha, Mohamed Fayçal Almi, Boualem Bendi
- [34] *“Levelized Cost and Levelized Avoided Cost of New Generation Resources in the Annual Energy Outlook 2019”*, U.S. Energy Information Administration (E.I.A.)
- [35] *“Renewable Power generation costs in 2018”*, IRENA (“International Renewable Energy Agency”)

- [36] *“Battery Storage for renewables: market status and technology outlook”, IRENA 2015*
- [37] *“Hydrogen from renewable power – Technology outlook for the energy transition”, IRENA 2018*
- [38] *International Energy Agency (IEA), Report – “Producing ammonia and fertilizers: new opportunities from renewables”*
- [39] *“Hydrogen transportation by pipelines”, I.A. Gondal, National University of Sciences & Technology, Rawalpindi, Pakistan*
- [40] *“The use of the natural-gas pipeline infrastructure for hydrogen transport in a changing market structure”, Dries Haeseldonckx, William D’haeseleer*
- [41] *“The use of natural gas pipeline network with different energy carriers”, Linlin Ma, Catalina Spataru*
- [42] *“Optimization of hybrid PV-wind system: Case study Al-Tafilah cement factory”, Jordan Loiy Al-Ghussain, Humayun Ahmed, Fahad Haneef*
- [43] *“Economic assessment of investment projects in the energy sector”, slides of Prof. Pierluigi Leone for “Thermal Design and Optimization” (course of Politecnico di Torino).*

APPENDIX A: Matlab code

The developed MATLAB code to verify the proper operation of the proposed optimal configuration of the pv-wind-storage system is presented in this section.

```
clear all
close all
clc

conf=[1 0;0.9 0.1;0.8 0.2;0.7 0.3;0.6 0.4;0.5 0.5;0.4 0.6;0.3 0.7;0.2 0.8;0.1 0.9;0
1]*Eload_mese;
vv=[1;2;3;4;5;6;7;8;9;10;11];
nwt=ceil(conf(:,1)/E1wt_mp);
npv=ceil(conf(:,2)/E1pv_mp);
P_wtssystem=nwt*3;
P_pvsystem=npv*0.3*1e-3;
ore=linspace(1,8760+24,8760+24)';

for zz=1:length(nwt)
for kk=1:length(npv)
    for tt=1:length(ore)
Egenerata_wt(tt,zz)=E1wt_h(tt)*nwt(zz)+E1pv_y*ff(tt)*npv(1);
Egenerata_pv(tt,kk)=E1wt_h(tt)*nwt(11)+E1pv_y*ff(tt)*npv(kk);
    end
end
end
Egenerata_wt1y=sum(Egenerata_wt);
Egenerata_pv1y=sum(Egenerata_pv);
tosavewt=[Egenerata_wt1y];
tosavepv=[Egenerata_pv1y];
Egenerata=Egenerata_wt+Egenerata_pv;
Egenerata_y=Egenerata_wt1y+Egenerata_pv1y;

C_1bat=1.3*1e-6;
sigma_day=0.14;
sigmah=sigma_day/24/100;
eff_carica=0.903;
eff_bat=0.95;
DoD=0.8;

Cn_storage=(vv(3)*diff)/(DoD*eff_bat);
```

```

nb=Cn_storage/C_1bat;
Cstorage_max=Cn_storage;
Cstorage_min=(1-DoD)*Cn_storage;

```

```
ii=1;
```

```
while ii<12
```

```

Cstorage(1,ii)=Cstorage_max(ii,1);
SOC(1,ii)=Cstorage(1,ii)/Cstorage_max(ii,1)*100;
Egenerata(1,ii)=Egenerata(1,ii);
conta(ii,1)=0;

```

```
for tt=2:length(ore)
```

```
if Egenerata(tt,ii)>Eload_h
```

```
    %FASE DI CARICA
```

```
    Cstorage(tt,ii)=Cstorage(tt-1,ii)*(1-sigmah)+(Egenerata(tt,ii)-Eload_h)*eff_carica;
```

```
if Cstorage(tt,ii)<Cstorage_max(ii,1)
```

```
    SOC(tt,ii)=Cstorage(tt,ii)/Cstorage_max(ii,1)*100;
```

```
else
```

```
    Cstorage(tt,ii)=Cstorage_max(ii,1);
```

```
    SOC(tt,ii)=Cstorage(tt,ii)/Cstorage_max(ii,1)*100;
```

```
end
```

```
end
```

```
if Egenerata(tt,ii)<Eload_h
```

```
    %FASE DI SCARICA
```

```
    Cstorage(tt,ii)=Cstorage(tt-1,ii)*(1-sigmah)-(Eload_h-Egenerata(tt,ii));
```

```
if Cstorage(tt,ii)>Cstorage_min(ii,1)
```

```
    SOC(tt,ii)=Cstorage(tt,ii)/Cstorage_max(ii,1)*100;
```

```
else
```

```
    Cstorage(tt,ii)=Cstorage_min(ii,1);
```

```
    SOC(tt,ii)=Cstorage(tt,ii)/Cstorage_max(ii,1)*100;
```

```
end
```

```
end
```

```
if SOC(tt,ii)==SOC(tt-1,ii) && Egenerata(tt,ii)==0
```

```
conta(ii,1)=conta(ii,1)+1;
```

```
end
```

```
if Cstorage(tt-1,ii)>Cstorage(tt,ii)
    Scarica(tt,ii)=Cstorage(tt-1,ii)-Cstorage(tt,ii);
    ScaricaMax=(max(Scarica)*1e3);
else
    Scarica(tt,ii)=0;
end
end
ii=ii+1;
end

tosave=[SOC];
tosaveC=[Cstorage];
save('SOC_optimization1.dat','tosave','-ascii');
save('Storage_optimization1.dat','tosaveC','-ascii');
```